Lattice model of equilibrium polymerization. V. Scattering properties and the width of the critical regime for phase separation

Kyunil Rah,[a] Karl F. Freed,[b] and Jacek Dudowicz
The James Franck Institute, The University of Chicago, Chicago, Illinois 60637
and Department of Chemistry, The University of Chicago, Chicago, Illinois 60637

Jack F. Douglas
Polymers Division, National Institute of Standards and Technology, Gaithersburg, Maryland 20899

(Received 12 January 2006; accepted 7 February 2006; published online 12 April 2006)

Dynamic clustering associated with self-assembly in many complex fluids can *qualitatively* alter the shape of phase boundaries and produce large changes in the scale of critical fluctuations that are difficult to comprehend within the existing framework of theories of critical phenomena for nonassociating fluids. In order to elucidate the scattering and critical properties of associating fluids, we consider several models of *equilibrium polymerization* that describe widely occurring types of associating fluids at equilibrium and that exhibit the well defined cluster geometry of linear polymer chains. Specifically, a Flory-Huggins-type lattice theory is used, in conjunction with the random phase approximation, to compute the correlation length amplitude ξ_o and the Ginzburg number Gi corresponding, respectively, to the scale of composition fluctuations and to a parameter characterizing the temperature range over which Ising critical behavior is exhibited. Our calculations indicate that upon increasing the interparticle association energy, the polymer chains become increasingly long in the vicinity of the critical point, leading naturally to a more asymmetric phase boundary. This increase in the average degree of polymerization implies, in turn, a larger ξ_o and a drastically reduced width of the critical region (as measured by Gi). We thus obtain insight into the common appearance of asymmetric phase boundaries in a wide range of "complex" fluids and into the observation of apparent mean field critical behavior even rather close to the critical point. © *2006 American Institute of Physics*. [DOI: 10.1063/1.2181138]

I. INTRODUCTION

While the theory of phase separation in "simple," nonassociating fluids has reached an advanced state and successfully explains the critical properties of these systems,[1–7] our understanding of the critical behavior of many "complex" fluids encountered in everyday practice is still rather limited. The literature is full of reports of "deviations" from ordinary critical behavior, especially in ionic fluids (ranging from colloidal, ionomer, and polyelectrolyte solutions to proteins, viruses, and DNA),[8–16] micelle forming liquids,[17] and other fluids exhibiting interparticle association. The latter systems are being increasingly subjected to quantitative investigation because of their importance for understanding fundamental biological processes involving protein aggregation and self-assembly and because of their many practical applications in commercial formulations of consumer products and in material processing.

In contrast to simple or nonassociating liquids, associating fluids commonly exhibit highly asymmetric phase boundaries, and, correspondingly, coexisting phases having disparate volumes (or compositions).[9,16,18,19] Indeed, the shapes of the phase boundaries in complex fluids are often reported to resemble those of polymer solutions.[15,19–21] Numerous studies have also indicated apparent mean-field critical exponents for these fluids for temperature ranges where simple fluids would exhibit Ising-type critical behavior.[8–16] However, increasingly refined measurements demonstrate that these associating fluids display Ising critical behavior at temperatures very close to the critical point, indicating that the width of the nonclassical critical region is actually much smaller than for simple fluids.[22–26] As frequently noted, the critical exponents switch sharply between their mean-field and Ising values in the narrow critical regime of these complex fluids,[9,11,22,27] a feature also characteristic of the critical behavior of polymer solutions.[28,29]

Recent simulations[30] provide insight into the physical origins of the critical properties of these complex fluids, although the theory of these systems remains relatively undeveloped. For example, simulations for an electrically neutral fluid of charged hard spheres (the "restricted primitive model") indicate that ion pairs form large scale dynamic polymeric structures at equilibrium and that ion pairing and subsequent polymerization of dipolar clusters strongly affect the critical properties of these fluids.[30] The presence of these dynamic clusters has long been suggested based on indirect experimental observations.[30] Simulations reveal that both charge valence and particle size asymmetries influence the character of the clustering (linear chains versus branched polymers) and that the tendency to form transient polymer structures is quite general in charged fluids.[31] The nature of

[a]Present address: Information and Electronic Materials Institute, LG Chem Research Park, 104-1 Munji-dong, Yuseong-gu, Daejeon, Korea 305-380.
[b]Electronic mail: k-freed@uchicago.edu

the clustering apparently simplifies when there is a large asymmetry in the ion sizes, and linear polymer chain clusters are highly prevalent in this limit.[32] Clustering also occurs, of course, in dipolar fluids where the dipolar particles exhibit a strong propensity to form chains at equilibrium with head-to-tail configurations.[33] These observations suggest that the critical properties of many associating fluids should resemble those for polymer solutions.[19–21] Once the prevalance for polymerization in these fluids is recognized, the differences in the width of the critical region and in the size of the critical fluctuations between complex and simple fluids become almost obvious. Our goal then lies in developing a theoretical description of this ubiquitous clustering phenomenon and of its impact on the critical and scattering properties of complex fluids.

We have recently shown that many thermodynamic properties (critical temperature, critical composition, osmotic compressibility,[34] etc.) of dipolar fluids can be *quantitatively* described by using a simple Flory-Huggins (FH) model of equilibrium polymerization.[32,35–37] Dipolar fluids are prototypical associating fluids, and their successful description by a FH-type approach represents a promising start for developing a general theory of associating fluids. However, this theory has not been developed to provide a complete description of critical properties, such as the correlation length or the width of the critical region and other basic critical properties that are helpful in comprehending the critical behavior of these associating fluids. The mean-field nature of this modeling is also an intrinsic limitation.

The present paper directly addresses itself to the problem of calculating the scattering properties of equilibrium polymer solutions, but our treatment is still limited to mean-field theory. Despite this restriction, we are able to compute the Ginzburg number (Gi) which delineates the size of the critical region for phase separation in solutions of polydisperse clusters that are generated by equilibrium polymerization. The calculations are performed for several models of equilibrium polymerization that exhibit different constraints on the polymerization process. These constraints regulate the degree of polymerization at low temperatures and the breadth of the polymerization transition,[38] and their influence on the criticality of these associating liquids is the subject of the present paper.

The analysis begins with the free association ($\mathcal{FA}$) polymerization model in which every particle (monomer) can promiscuously associate with any other particle without any condition other than physical proximity. We then analyze the case where polymerization is initiated by a thermally activated process ($\mathcal{A}$ model) that has a relatively low probability. The small equilibrium constant for activation acts as a constraint on further polymerization and leads to a much sharper polymerization transition as a function of temperature since there are fewer activated species competing for available monomer "mates." This thermal activation constraint is also found to produce substantial changes in the critical properties of this class of associating fluids, as discussed below. The polymerization equilibrium can likewise be modulated by the introduction of a chemical initiator (the $\mathcal{I}$ or "living polymerization" model),[38–41] which plays a role similar to that of thermally activated species. Since thermal activation and chemical initiation similarly affect the critical properties of equilibrium polymers, we restrict the discussion below to the illustrative case of the $\mathcal{A}$ model. The case of a large activation equilibrium constant is not considered since this case leads to fairly short chains[38] and, thus, the critical properties of these fluids are only slightly perturbed compared to simple liquids. Our initial representative calculations focus on systems for which the extent of polymerization becomes appreciable to emphasize the qualitative consequences of strong association on critical properties.

Another important factor analyzed in our calculations is the impact of chain stiffness on the critical properties of equilibiurm polymerization solutions. Chain rigidity influences the critical behavior of ordinary polymer solutions and must likewise affect the critical behavior of fluids undergoing equilibrium polymerization. Much of our discussion is confined to Gaussian and wormlike polymer chain models as extreme limits. The computation of Gi and the correlation length amplitude for these model associating polymer solutions requires the evaluation of the square gradient coefficient κ that describes the interfacial free energy cost of creating inhomogeneties in the polydisperse polymer solutions.

Section II briefly reviews the essential thermodynamic characteristics of models of equilibrium polymerization, focusing on quantities closely related to the critical properties of associating solutions. Section III describes the theoretical background for the basic scattering quantities that are required for computing the Ginzburg number. Illustrative calculations of the phase boundaries and the influence of association on both critical and scattering properties, as well as on the Ginzburg number, are summarized in Sec. IV.

II. FLORY-HUGGINS THEORY OF EQUILIBRIUM POLYMERIZATION

Our recent papers[38–41] develop a comprehensive theory of equilibrium polymerization. The theory describes the basic thermodynamic and critical properties of polydisperse polymer solutions, the competition between polymerization and phase separation, and the characteristic rounding for this type of thermodynamic clustering transition. The properties treated include the average chain length L, extent of polymerization Φ, Helmholtz free energy F, configurational entropy S, specific heat C_V, polymerization transition temperature T_p, osmotic pressure Π, second and third virial coefficients A_2 and A_3, and the critical temperature T_c and critical composition ϕ_c for phase separation. This systematic treatment has been derived for three general models of association: a model with unrestricted equilibrium polymerization in which all particles can associate democratically at equilibrium (termed the $\mathcal{FA}$ model), a model in which the particles must become thermodynamically activated to initiate polymerization ($\mathcal{A}$ model), and finally a model in which chain growth is induced by a chemical initiator ($\mathcal{I}$ model).[38] This basic classification scheme for equilibrium polymerization follows that introduced long ago by Tobolsky and Eisenberg[42] and encompasses the main classes of equilibrium polymerization encountered in practice.

The present paper extends our theory to the description of the scattering and critical properties of equilibrium polymerization systems by considering quantities such as the structure factor $S(q)$, correlation length amplitude ξ_o, width of the critical regime, Ginzburg number Gi, etc. We briefly review those main theoretical results for the $\mathcal{FA}$ and $\mathcal{A}$ models that are required in developing the present extension of the theory for the critical behavior of associating fluids.

A. Free association model

The $\mathcal{FA}$ system is composed of n_s solvent molecules and n_1^o monomers of species M that can "freely associate" with polymers once the free energy for this process is negative. The resulting polymers form and disintegrate in dynamic equilibrium. Chain growth may proceed either by the addition of a single monomer or by the linkage of two chains. Chains may break in the middle, or segments may dissociate from the chain ends. These two modes of polymerization and depolymerization can be represented by the single kinetic equation[38]

$$M_j + M_k \rightleftharpoons M_{j+k}, \quad j,k = 1,2,\ldots,\infty. \tag{1}$$

The constant volume system is described using the standard Flory-Huggins lattice model in which single site occupancy constraints apply to solvent molecules and to all monomers (unreacted monomers and those present in polymers). The total number N_l of lattice sites is expressed in terms of the numbers $\{n_i\}$ of molecules of the individual species M_i as

$$N_l = n_s + \sum_{i=1}^{\infty} i n_i = n_s + n_1^o. \tag{2}$$

Equation (2) reflects the underlying assumptions of incompressibility and equal volumes for solvent molecules and for monomers of the associating species, assumptions recently lifted in a theory for the pressure dependence of equilibrium polymerization.[43] Equation (2) can be converted to the alternative form of the mass conservation condition,

$$\sum_{i=1}^{\infty} \phi_i = \phi_1^o, \tag{3}$$

that relates the volume fractions $\{\phi_i = i n_i / N_l\}$ of the polymer species $\{M_i\}$ to the volume fraction ϕ_1^o of monomers before polymerization.[44] The equilibrium constant K_p for the polymerization reaction in Eq. (1) is assumed to be same for all j and k and, thus, is expressed in terms of a single free energy Δf_p of polymerization as $K_p = \exp(-\Delta f_p / k_B T)$, with k_B designating Boltzmann's constant and T being the absolute temperature. For simplicity, all monomers are assumed to interact identically with the solvent molecules, regardless of whether they are unpolymerized (M_1) or belong to polymerized species M_i ($i \geqslant 2$), which, in turn, implies the presence of a single monomer-solvent interaction parameter χ.

Under the above assumptions, the equilibrium distribution of the volume fractions $\{\phi_i\}$ is solely dictated by the initial monomer concentration ϕ_1^o, the temperature T, and the energy Δh_p and entropy Δs_p of polymerization,[38]

$$\phi_i = i C A^i, \quad i \geqslant 2, \quad A \equiv \phi_1 K_p, \quad C \equiv z/(2\alpha K_p), \tag{4}$$

where the coefficient α equals $(z-1)$ and 1 for fully flexible and stiff chains, respectively.[38,45] Substituting Eq. (4) into Eq. (3) and performing all summations (with the constraint $0 < A < 1$) yield the relation between ϕ_1^o and ϕ_1,

$$\phi_1^o = \phi_1 + \frac{C A^2 (2 - A)}{(1 - A)^2}, \tag{5}$$

where the quantity $A \equiv A(\phi_1^o, T)$ is determined numerically from Eq. (5) for given T, ϕ_1^o, Δh_p, and Δs_p.

The extent of polymerization Φ (the fraction of monomers converted into polymers) and the average chain length L are basic properties of equilibrium polymerization solutions and are likewise functions of T, ϕ_1^o, Δh_p, and Δs_p through

$$\Phi \equiv \frac{\phi_1^o - \phi_1}{\phi_1^o} = \frac{1}{\phi_1^o} \frac{C A^2 (2 - A)}{(1 - A)^2} \tag{6}$$

and

$$L \equiv \frac{\sum_{i=1}^{\infty} \phi_i}{\sum_{i=1}^{\infty} \phi_i / i} = \frac{\phi_1^o}{\phi_1^o - [C A^2/(1 - A)^2]}. \tag{7}$$

A plot of $\Phi(T)$ versus T exhibits an inflection point, and the temperature T_Φ at which the derivative $\partial^2 \Phi / \partial T^2 |_{\phi_1^o}$ vanishes is often identified by experimentalists with the polymerization transition temperature T_p. The variation of T_p with ϕ_1^o is termed the "polymerization transition line" and provides a rough criterion for delineating the thermodynamic boundary between polymer rich and monomer rich states. This interpretation is less adequate for the $\mathcal{FA}$ model where the polymerization transition is broad. The temperature T_Φ is generally distinct[38] from T_p where the specific heat has a maximum. Both of these temperatures provide valuable information about the polymerization transition, and the gap between these temperatures represents a measure of how much the transition is rounded.[41]

The Helmholtz free energy F is the basic thermodynamic property of the system, and in contrast to $\{\phi_i\}$, Φ, and L, F also depends on the strength ϵ_{FH} of the effective monomer-solvent interactions,

$$\frac{F}{N_l k_B T} = (1 - \phi_1^o)\ln(1 - \phi_1^o) + \phi_1^o \ln \phi_1 + (1 - \phi_1^o)\phi_1^o \chi + \frac{C A^2}{(1 - A)^2}, \tag{8}$$

where the dimensionless monomer-solvent Flory-Huggins interaction parameter $\chi = \epsilon_{\mathrm{FH}}/T$ arises within FH theory as a purely energetic quantity that is inversely proportional to temperature.[46] The osmotic pressure Π of the associating solution is evaluated from the Helmholtz free energy F as

$$\frac{\Pi a^3}{k_B T} = -\frac{v_{\text{cell}}}{k_B T}\left.\frac{\partial F}{\partial V}\right|_{T,n_1^o}$$

$$= -\ln(1-\phi_1^o) - (\phi_1^o)^2\chi - \frac{CA^2}{(1-A)^2}, \tag{9}$$

with $v_{\text{cell}}=V/N_l$ being the volume associated with a single lattice site.

The condition for the existence of a stable homogeneous phase is given by the simple form

$$\left.\frac{\partial^2 F/(N_l k_B T)}{\partial \phi_1^{o2}}\right|_{N_l,T} > 0,$$

while the vanishing of the second derivative of F with respect to ϕ_1^o defines the constant volume spinodal curves $T=T(\phi_1^o)$ as the solution of the equation

$$\frac{1}{\phi_1^o + [2CA^2/(1-A)^3]} + \frac{1}{1-\phi_1^o} - 2\chi = 0, \tag{10}$$

where again the quantity $A \equiv A(\phi_1^o, T)$ emerges from the solution to Eq. (5).

An extremum of the spinodal curve identifies the critical temperature T_c and critical composition $\phi_c \equiv (\phi_1^o)_c$. Knowledge of these critical parameters, in conjunction with Eq. (9), enables calculating the (mean-field) critical osmotic compressibility factor $Z_c=\Pi_c a^3/(k_B T_c \phi_c)$, another important thermodynamic quantity for solutions of associating species.

B. Activated equilibrium polymerization

The simplest model of activated polymerization is described by the reaction scheme,[47]

$$M_1 \rightleftharpoons M_1^*, \tag{11}$$

$$M_1^* + M_1 \rightleftharpoons M_2, \tag{12}$$

$$M_i + M_1 \rightleftharpoons M_{i+1}, \quad i = 2,3,\ldots,\infty, \tag{13}$$

where the activated species M_1^* reacts only with nonactivated monomers M_1 to form dimers, but does not participate in the succesive chain propagation processes. An alternative model, in which dimers are formed by linking two activated monomers M_1^* and chain growth occurs exclusively through the addition of M_1^* to the resulting polymers, is mathematically isomorphic[38] to that described by Eqs. (11)–(13). The simplest model of Eqs. (11)–(13) is further specified by designating $\Delta f_a=\Delta h_a - T\Delta s_a$ and $\Delta f_p=\Delta h_p - T\Delta s_p$ as the free energies of activation and polymerization, respectively. In order to minimize the number of parameters, both the enthalpies Δh_p and entropies Δs_p associated with dimer formation [Eq. (12)] and with the propagation process [Eq. (13)], respectively, are taken as identical. As for the $\mathcal{FA}$ model, all monomers (unpolymerized and those in polymers) are treated as interacting identically with the solvent.

The distribution of volume fractions $\{\phi_i\}$ for all species i,

$$\phi_i = iCA^i, \quad i \geqslant 2, \quad A \equiv \phi_1 K_p, \quad C \equiv zK_a/(2\alpha K_p), \tag{14}$$

formally resembles that derived for the $\mathcal{FA}$ model [see Eq. (5)], except for the appearance of the volume fraction ϕ_1^* of the activated monomers,

$$\phi_1^* = \phi_1 K_a, \quad \text{with } K_a = \exp(-\Delta f_a/k_B T).$$

While the quantity A in Eq. (14) is defined as in Eq. (4), the prefactor C in Eq. (14) departs from its definition in Eq. (4) for the $\mathcal{FA}$ model by the presence of the equilibrium constant K_a for activation. This formal identity between Eqs. (4) and (14) does not imply, however, that A and $\{\phi_i\}$ have similar values for these two models since the mass conservation constraint for the activated association model,

$$\phi_1^o = \phi_1[1+K_a] + \frac{CA^2(2-A)}{(1-A)^2}, \tag{15}$$

contains an extra term $\phi_1^*=\phi_1 K_a$ that is absent in Eq. (5).

The definitions of the extent of polymerization Φ and the average degree of polymerization L explicitly include the presence of activated monomers,

$$\Phi \equiv \frac{\phi_1^o - \phi_1 - \phi_1^*}{\phi_1^o} = \frac{1}{\phi_1^o}\frac{CA^2(2-A)}{(1-A)^2} \tag{16}$$

and

$$L \equiv \frac{\phi_1^* + \Sigma_{i=1}^{\infty}\phi_i}{\phi_1^* + \Sigma_{i=1}^{\infty}(\phi_i/i)} = \frac{\phi_1^o}{\phi_1^o - [CA^2/(1-A)^2]}, \tag{17}$$

but the right hand sides of Eqs. (16) and (17) are formally the same as those in Eqs. (6) and (7), respectively. A more detailed analysis of Eqs. (16) and (17) reveals that that both Φ and L are no longer generally monotonic functions of temperature when an activated process is present.[38]

The Helmholtz free energy of the system can be converted into a form that does not explicitly contain the volume fraction ϕ_1^* and that is *formally identical* to Eq. (8),

$$\frac{F}{N_l k_B T} = (1-\phi_1^o)\ln(1-\phi_1^o) + \phi_1^o \ln\phi_1 + (1-\phi_1^o)\phi_1^o\chi + \frac{CA^2}{(1-A)^2}. \tag{18}$$

Short range van der Waals interactions are represented in Eq. (18) [as in Eq. (8)] by a single interaction parameter χ that describes the average effective interactions between the solvent and monomers of the associating species M.

The formally identical expressions for the free energy F for the $\mathcal{FA}$ and $\mathcal{A}$ models imply a common expression for the osmotic pressure [see Eq. (9)],

$$\frac{\Pi v_{\text{cell}}}{k_B T} = -\ln(1-\phi_1^o) - (\phi_1^o)^2\chi - \frac{CA^2}{(1-A)^2},$$

and for the spinodal stability condition [see Eq. (10)],

$$\frac{1}{\phi_1^o + [2CA^2/(1-A)^3]} + \frac{1}{1-\phi_1^o} - 2\chi = 0.$$

As already mentioned, this commonality does not lead to the same values of Π, T_c, ϕ_c, etc., in these two models due to the different mass conservation equations determining A.

III. CRITICAL PROPERTIES OF EQUILIBRIUM POLYMER SOLUTIONS

The formal expansion of the specific Helmholtz free energy $f=F/N_l$ around the critical point for a homogeneous equilibrium polymerization solution,

$$\frac{f}{k_BT} = \frac{f_c}{k_BT_c} + a_{10}\eta + \frac{1}{2}a_{21}\eta^2\tau + \frac{1}{3!}a_{31}\eta^3\tau + \frac{1}{4!}a_{40}\eta^4 + \cdots, \tag{19}$$

is derived[48] assuming that f is an analytic function of the order parameter $\eta \equiv \phi - \phi_c$ [defined as the difference between the actual composition $\phi \equiv \phi_1^o$ and the critical composition $\phi_c \equiv (\phi_1^o)_c$] and of the reduced temperature $\tau \equiv (T-T_c)/T$. The coefficients a_{10}, a_{21}, a_{31}, and a_{40} in Eq. (19) are derivatives of the specific Helmholtz free energy, evaluated at the critical point (i.e., at $\phi=\phi_c$ and $T=T_c$),

$$a_{10} = \left.\frac{\partial(f/k_BT)}{\partial\eta}\right|_{\phi_c,T_c}, \tag{20}$$

$$a \equiv a_{2,1} = \left.\frac{\partial^3(f/k_BT)}{\partial\eta^2\partial\tau}\right|_{\phi_c,T_c}, \tag{21}$$

$$a_{31} = \left.\frac{\partial^4(f/k_BT)}{\partial\eta^3\partial\tau}\right|_{\phi_c,T_c}, \tag{22}$$

$$b \equiv a_{4,0} = \left.\frac{\partial^4(f/k_BT)}{\partial\eta^4}\right|_{\phi_c,T_c}, \tag{23}$$

and f_c is the specific free energy f of Eq. (8) [or Eq. (18)] at the critical point, i.e., $f_c \equiv f(\phi=\phi_c, T=T_c)$.

Contributions from fluctuations of the order parameter are appended to Eq. (19) by the addition of a square gradient term,[2] which transforms Eq. (19) into the free energy expansion,

$$\frac{f}{k_BT} = \frac{f_c}{k_BT_c} + a_{10}\eta + \frac{1}{2}a\eta^2\tau + \frac{1}{3!}a_{31}\eta^3\tau + \frac{1}{4!}b\eta^4 + \frac{1}{2}\kappa_c|\nabla\eta|^2 + \cdots, \tag{24}$$

where the order parameter $\eta \equiv \eta(\mathbf{r})$ now is spatially varying and the square gradient coefficient κ is evaluated at the critical point, i.e., $\kappa_c = \kappa(\phi=\phi_c, T=T_c)$.

A. Basic scattering properties

We next discuss basic relations describing the long wavelength scattering properties of equilibrium polymerization solutions. The coefficient κ, whose evaluation for polydisperse polymer solutions is described in Sec. III C, is determined from the expansion of the structure factor $S(q)$ in the small angle limit of $q=0$,

$$\frac{1}{S(q)} = \frac{1}{S(0)} + \kappa q^2 + \cdots. \tag{25}$$

Moreover, κ is related to the static correlation length ξ, which is defined through the Ornstein-Zernicke equation[2]

$$S(q) = \frac{S(0)}{1+\xi^2q^2}, \quad q \to 0, \tag{26}$$

by

$$\kappa = \frac{\xi^2}{S(0)}. \tag{27}$$

The mean field static correlation length ξ scales with the reduced temperature τ according to the (mean field) defining relation,

$$\xi = \xi_o|\tau|^{-1/2}, \tag{28}$$

and the correlation length amplitude ξ_o is independent of temperature. The mean field sum rule $\xi^2 \sim S(0)$ in Eq. (27) implies that ξ_o controls both the intensity $[S(0)]$ and the scale (ξ) of composition fluctuations.[48] More generally, ξ scales as $\xi \sim |\tau|^{-\nu}$ with $\nu=0.630$ in the Ising critical regime. The long wavelength limiting structure factor $S(0)$ is proportional to the isothermal osmotic compressibility $(1/\phi_1^o)(\partial\phi_1^o/\partial\Pi)$ and near the critical point scales with τ as

$$S(0,\phi_c,\tau) = \Gamma_c|\tau|^{-\gamma}, \tag{29}$$

where $\Gamma_c \equiv \Gamma(\phi_c) = 1/|a|$ plays the role of the critical amplitude for $S(0)$ [with a given by Eq. (20)] and where $\gamma=1$ and 1.239 for the mean field and three-dimensional (3D) Ising critical behaviors,[5,6] respectively. Combining Eqs. (27)–(29) yields the "sum rule" relating κ, ξ_o, and Γ within a mean-field approximation,

$$\kappa = \xi_o^2/\Gamma. \tag{30}$$

B. Ginzburg number

The temperature ranges over which mean field and Ising-type critical behaviors apply are expressed in terms of the Ginzburg number Gi.[1] This quantity provides an estimate of the magnitude of the reduced temperature τ at which the crossover from mean field to Ising-type behaviors occurs. Importantly, *Gi can be obtained from mean field theory* through a direct determination of the condition that the fluctuation contribution to the long wavelength scattering factor $S(0)$ is comparable to the mean field contribution. We have introduced[48] a refined Ginzburg criterion that distinguishes three temperature ranges, the mean field and Ising scaling regimes, as well as an intermediate "crossover regime" of criticality that separates the first two. Specifically, our previous analysis[48] indicates that mean field theory holds for $\tau \geqslant 10$ Gi, while Ising critical behavior corresponds to $\tau \leqslant \mathrm{Gi}/10$. The range $\mathrm{Gi}/10 < \tau < 10$ Gi describes the crossover regime, so that $\tau \simeq$ Gi lies in the middle of this reduced temperature range. The Ginzburg number Gi for a fluid un-

dergoing an equilibrium polymerization is expressed as[48]

$$\mathrm{Gi} = \frac{b^2}{64\pi^2|a|(\kappa_c^*)^3}, \tag{31}$$

where the coefficients a and b are given by Eqs. (19) and (20), respectively, and $\kappa_c^* \equiv \kappa_c/a_{\mathrm{cell}}^2$ is the dimensionless square gradient coefficient $\kappa/a_{\mathrm{cell}}^2$ evaluated at the critical point, with a_{cell} being the lattice constant. The Ginzburg number Gi can be presented alternatively as

$$\mathrm{Gi} = \frac{b^2\Gamma_c^4}{64\pi^2(\xi_{o,c}^*)^6}, \tag{32}$$

where $\xi_{o,c}^* \equiv \xi_{o,c}/a_{\mathrm{cell}}$ is the dimensionless correlation length amplitude ξ_o/a_{cell} evaluated at the critical composition ϕ_c. Section III C describes the estimation of κ_c^* for an equilibrium polymerization solution.

C. Square gradient coefficient κ

According to the random phase approximation (RPA) theory,[49] the structure factor $S(q)$ for an incompressible solution of monodisperse polymer species in a (structured) solvent is given by

$$\frac{1}{S(q)} = \frac{1}{i\phi P_i(q)} + \frac{1}{(1-\phi)P_s(q)} - 2\chi(q), \tag{33}$$

where ϕ is the volume fraction of polymers, i designates the polymerization index (i.e., the number of monomers in a single chain), $P_i(q)$ and $P_s(q)$ are the form factors for a single polymer chain and a solvent molecule, respectively, and $\chi(q)$ is a linear combination of the Fourier transforms $c_{\alpha\beta}(q)$ of the direct correlation functions $c_{\alpha\beta}(r)$.[50] Notice that Eq. (33) describes a system in which a solvent molecule and individual monomer of a polymer chain have the same volumes (and thus occupy single lattice sites in the lattice model). This simplifying assumption can readily be lifted, but is invoked only to keep the number of parameters to a minimum.

The extension of Eq. (33) to a solution of polydisperse polymer chains in a (structured) solvent involves introducing a summation in the denominator of the first term on the right hand side of Eq. (33) over all sizes i of the equilibrium polymers.[49] The resulting generalized RPA expression for $S(q)$ emerges as

$$\frac{1}{S(q)} = \frac{1}{\Sigma_{i=1}^{\infty}[i\phi_i P_i(q)]} + \frac{1}{(1-\phi)P_s(q)} - 2\chi(q), \tag{34}$$

where $P_i(q)$ now denotes the structure factor for an individual i-mer, ϕ_i is its volume fraction, and where the shorthand notation $\phi \equiv \phi_1^o = \phi_1^* + \Sigma_i^{\infty}\phi_i$ is employed. [The thermodynamic $q \to 0$ limit of Eq. (34) has been discussed previously by Stockmayer.[34]] The form factors $P_i(q)$ and $P_s(q)$ of Eq. (34) are related to the corresponding radii of gyration $R_{g,i}$ and $R_{g,s}$ of a polymer and a solvent molecule, respectively, through the well-known long wavelength limit expressions

$$P_i(q) = 1 - \tfrac{1}{3}(R_{g,i})^2q^2 + \mathcal{O}(q^4) + \cdots \tag{35}$$

and

$$P_s(q) = 1 - \tfrac{1}{3}(R_{g,s})^2q^2 + \mathcal{O}(q^4) + \cdots. \tag{36}$$

Equations (35) and (36) are valid for arbitrary shaped objects and, thus, apply to polymers as well as solvent molecules and monomer species. Since the square gradient coefficient κ is defined as the coefficient of the q^2 term in the expansion,

$$\frac{1}{S(q)} = \frac{1}{S(0)} + \kappa q^2 + \mathcal{O}(q^4) + \cdots, \tag{37}$$

we combine Eqs. (34)–(37) to obtain an explicit expression for κ,

$$\kappa^* \equiv \frac{\kappa}{a_{\mathrm{cell}}^2} = \frac{(1/3)\Sigma_{i=1}^{\infty}[i\phi_i(R_{g,i}^*)^2]}{(\Sigma_{i=1}^{\infty}i\phi_i)^2} + \frac{(1/3)(R_{g,s}^*)^2}{1-\phi},$$
$$R_{g,i}^* \equiv \frac{R_{g,i}}{a_{\mathrm{cell}}}, \quad R_{g,s}^* \equiv \frac{R_{g,s}}{a_{\mathrm{cell}}}, \tag{38}$$

where the sum over i includes the activated monomers (if they are present in the system). Reduced variables are used in Eq. (38) for both κ and the radii of gyration of all scattering species and are defined in terms of the lattice cell dimension a_{cell} which is specified below. While the estimation of $R_{g,i}$ for polymer chains ($i \geqslant 2$) can be performed following standard methods, the determination of the monomer $R_{g,i=1}$ and solvent molecule $R_{g,s}$ requires special consideration.

To evaluate $R_{g,i=1}$ and $R_{g,s}$, we consider a reference monomer-solvent mixture in which monomers are not polymerized. The structure factor $S(q)$ for this system is also described by the Ornstein-Zernicke relation

$$S(q) \sim 1/(1+\xi^2q^2). \tag{39}$$

For an athermal ($\chi=0$) mixture, $S(q)$ scales as

$$S(q) \sim 1/[1+(1/3)R_g^2q^2], \tag{40}$$

where R_g denotes the radius of gyration for the monomeric scattering species. The mean field Eq. (40) is valid only when both the scattering species components have the same volumes and shapes. The correspondence of Eqs. (39) and (40) under athermal condition [i.e., far from the critical point where $\xi_c = \xi_{o,c}$; see Eq. (28)] implies the identification of the square of the correlation length amplitude $\xi_{o,c}$ with $(1/3)R_g^2$ for this unpolymerized system. The quantity $\xi_{o,c}$ reflects a minimum cutoff scale for composition fluctuations, and we therefore define this parameter as the basic unit of length in our lattice model. Taking $\xi_{o,c} = a_{\mathrm{cell}}$ leads to the simple dimensionless estimate for the radii of gyration of monomers and solvent molecules,

$$R_{g,i=1}^* = R_{g,s}^* = \sqrt{3}. \tag{41}$$

The determination of the radii of gyration $\{R_{g,i\geqslant 2}\}$ for polymer chains ($i \geqslant 2$) requires the adoption of a model for the chain conformational statistics. According to the ideal Gaussian chain model, the radius of gyration is simply proportional to the product of the Kuhn length l_K and the square root of the polymerization index i,

$$(R_{g,i})^2 = \tfrac{1}{6} i l_K^2. \tag{42}$$

A reasonable estimate of the Kuhn length l_K^*,

$$l_K^* \equiv \frac{l_K}{a_{\text{cell}}} = 2R_{g,i=1}^* = 2\sqrt{3}, \tag{43}$$

can be obtained from the assumption that l_K represents the approximate center-to-center distance between two touching (spherical) monomers bonded to each other in the polymer chain. Note that the Gaussian chain approximation of Eq. (42) underestimates $R_{g,i}$ for relatively short random flight chains.

The substitution of Eqs. (41)–(43) into Eq. (38) simplifies the latter to the rather compact form

$$\kappa^* = \frac{\phi_1 + \phi_1^* + (2/3)s_1}{s_0^2} + \frac{1}{1-\phi}, \tag{44}$$

where the sums s_0 and s_1,

$$s_0 \equiv \phi_1 + \phi_1^* + \sum_{i=2}^{\infty} i\phi_i = \frac{A}{K_p} + \frac{A}{K_p}K_a + \frac{CA^2(A^2 - 3A + 4)}{(1-A)^3}, \quad A \equiv \phi_1 K_p \tag{45}$$

and

$$s_1 \equiv \sum_{i=2}^{\infty} i^2\phi_i = \frac{CA^2(-A^3 + 4A^2 - 5A + 8)}{(1-A)^4}, \tag{46}$$

are evaluated by using Eq. (5) of Sec. II. Equations (44)–(46) apply to both the $\mathcal{FA}$ and $\mathcal{A}$ models of equilibrium polymerization. In the former case, the concentation ϕ_1^* of the activated monomers or the equilibrium constant K_a for the activation process is set to zero in Eqs. (44) and (45). The value κ_c^* of κ^* at the critical point is obtained from Eq. (44) by setting $\phi_1 = \phi_{1,c}$, $\phi_1^* = \phi_{1,c}^*$, $\phi = \phi_c$, and $T = T_c$,

$$\kappa_c^* = \kappa^*(\phi_1 = \phi_{1,c}, \phi_1^* = \phi_{1,c}^*, \phi = \phi_c, T = T_c), \tag{47}$$

where the subcripts c on ϕ_1, ϕ_1^*, ϕ, and T indicate that these quantities are evaluated at the critical point.

The radius of gyration for the wormlike chain model is a more complicated function of the persistence length $1/(2\lambda)$ and the bond length l_b, and the counterpart of Eq. (44) is derived in Appendix A for this model.

Andrews *et al.*[51] have previously applied the RPA theory to describe scattering properties of living polymer solutions within the context of an $n \to 0$ spin polymer-magnet analogy that corresponds to the $\mathcal{I}$ model of equilibrium polymerization.[38–41] These computations compare reasonably well to experiments for living poly(α-methylstyrene) in a good solvent (deuterated tetrahydrofuran), but critical fluctuation effects associated with phase separation are not emphasized in this work. In particular, Andrews *et al.*[51] do not expand the free energy about the critical point as in our Eq. (19) and do not consider the critical properties relating to phase separation. They focus instead on good solvent regime where the primary contribution to the wave vector (q) dependence of the scattering arises from the polymers alone. Andrews *et al.*[51] also study the screening of excluded volume interactions that naturally arise in such good solvents. These excluded volume screening effects cannot be described by mean field theory and involve a different type of fluctuation effects (polymer excluded volume) than the kind encountered in phase separation.

Although the calculations of Andrews *et al.* are based on an abstract polymer-magnet analogy that is sometimes difficult for us to follow, we have shown elsewhere that $S(0)$ from this formalism essentially coincides with our mean field theory approximation for $S(0)$.[41] On the other hand, we find their lengthy RPA expression for the correlation length $\xi(T)$ rather difficult to understand since their expression exhibits no *explicitly identifiable relation* to the radii of gyration of the assembling polymer chains nor to the size distribution of the chains. Clearly these quantities must be explicitly described to treat chain flexibility, e.g., the wormlike chain model.

D. Ginzburg number for monomer-solvent reference system

The reference system for the current analysis of equilibrium polymerization solutions is chosen as the monomer-solvent mixture in which the monomers do not polymerize, but still interact with solvent molecules through the effective interaction energy ϵ_{FH}. Equation (32) for the Ginzburg number for this system may be written as

$$\text{Gi} = \frac{b^2}{64\pi^2 a^4 (\xi_{o,c}^*)^6} \tag{48}$$

and involves the correlation length amplitude $\xi_{o,c}$ and the thermodynamic derivatives a and b defined by Eqs. (21) and (23), respectively, for the unpolymerized system. These derivatives are readily evaluted within the FH theory as

$$a \equiv \left.\frac{\partial^3 (f/k_B T)}{\partial \eta^2 \partial \tau}\right|_{\phi_c, T_c} = \frac{2\epsilon_{\text{FH}}}{\epsilon_{\text{FH}}/2} = 4 \tag{49}$$

and

$$b \equiv \left.\frac{\partial^4 (f/k_B T)}{\partial \eta^4}\right|_{\phi_c, T_c} = \frac{2}{\phi_c^3} + \frac{2}{(1-\phi_c)^3} = 32, \tag{50}$$

where the conditions for the critical composition ϕ_c and critical temperature T_c, i.e., $\phi_c = 0.5$ and $T_c = (1/2)\epsilon_{\text{FH}}$, have been utilized. Interestingly, the derivative a coincides with the mean-field estimate of the ratio of the theta temeperature to the critical temperature for a monomer-solvent system. The remaining quantity $\xi_{o,c}^*$ of Eq. (48) is already known through the identification of $\xi_{o,c}$ with the lattice constant a_{cell}.

The square gradient coefficient κ_c for the reference system can be determined as a special limit of Eq. (38),

$$\kappa_c^* \equiv \frac{\kappa_c}{a_{\text{cell}}^2} = \frac{1}{3}\left[\frac{(R_{g,i=1})^2}{\phi_c} + \frac{(R_{g,s})^2}{1-\phi_c}\right] = \frac{1}{3}\left[\frac{3}{(1/2)} + \frac{3}{(1/2)}\right] = 4, \tag{51}$$

upon use of the radii of gyration for a monomer and solvent molecule from Eq. (41). The reduced correlation length am-

plitude $\xi^*_{o,c} \equiv \xi_{o,c}/a_{\text{cell}}$, computed from Eq. (30), equals unity,

$$\xi^*_{o,c} = \sqrt{\kappa^*_c/a} = 1, \tag{52}$$

consistent with our previous definition. Finally, the Ginzburg number Gi for the monomer-solvent reference system follows from Eq. (48) as

$$\text{Gi} = \frac{1}{16\pi^2} \simeq 0.0063, \tag{53}$$

a value that is not only consistent with the typical order of magnitude for Gi for binary mixtures of small molecules and for single component simple fluids [$\text{Gi} \sim \mathcal{O}(0.01)$],[2] but that also coincides with a numerical estimate[2] of Gi=0.006 for a lattice model monomer-solvent system based on simulation data of Mackie *et al.*[52] Our estimate of the reduced temperature $\tau \equiv (T-T_c)/T_c$ range over which Ising-type scaling is exhibited [$\text{Gi}/10 \sim \mathcal{O}(0.001)$] also agrees with typical values cited for nonquantum small molecule fluids.[53]

E. Quartic coupling constant *b*

Equation (32) indicates that Gi, and thus the width of the critical region in which Ising critical behavior is exhibited, depends on three physical quantities: the parameters Γ_c and $\xi_{c,o}$ that characterize the amplitude and the spatial scale of composition fluctuations, respectively, and the quartic coupling constant b from the expansion of the free energy density [see Eq. (23)]. The first two quantities have an obvious physical interpretation, but b evidently is a more abstract quantity whose variation with particle association is difficult to understand intuitively. A general expression for b in terms of molecular parameters would provide a powerful tool for estimating the width of the critical region for complex fluids since Γ_c and $\xi^*_{o,c}$ may be determined from measurements or simulations.

A fluid undergoing equilibrium polymerization with a strongly directional association enthalpy Δh_p can basically be considered to be a polydisperse polymer solution. (Certainly, a snapshot of such a fluid would give this appearance at any point in time.) This viewpoint suggests that it might be possible to estimate b from the Flory-Huggins theory of monodisperse polymer solutions in which the polymers are *permanent* rather than dynamic. This FH estimate of b is designated as b_{FH} and is compared below with the b evaluated from our equilibrium polymerization theory to gain insights into the qualitative meaning of b.

The FH expression for b is obtained by combining the definition of b from Eq. (23) with the FH relations for the free energy and the critical composition of monodisperse polymer solutions,[54]

$$b_{\text{FH}} = 2N^{1/2}(1+N^{-1/2})^4, \tag{54}$$

where N denotes the polymerization index. For long polymer chains ($N \to \infty$), b_{FH} scales as $b_{\text{FH}} \sim N^{1/2}$, so that b is expected to increase as a power law of the average degree of polymerization L when particle association is prevalent. The relation betwen b and L at the critical point (L_c) is examined in the next section. Table I summarizes other critical properties of monodisperse polymer solutions that are useful in our comparative analysis below.

TABLE I. The critical parameters of monodisperse polymer solutions.

ϕ_c	$\frac{1}{1+\sqrt{N}} \sim N^{-1/2}$	Reference 54
T_c	$2\epsilon_{\text{FH}}\left(\frac{\sqrt{N}}{1+\sqrt{N}}\right)^2 \sim 2\epsilon_{\text{FH}}$	Reference 54
R^*_g	$\sqrt{N/6}\,l^*_K$	
a	$(1+N^{-1/2})^2 \sim 1$	Reference 52
b	$2\sqrt{N}(1+N^{-1/2})^4 \sim 2N^{1/2}$	Reference 52
κ^*_c	$(1+\sqrt{N})[(l^*_K)^2/18+N^{-1/2}] \sim N^{1/2}$	
$\xi^*_{o,c}$	$\frac{\sqrt{N}}{\sqrt{1+\sqrt{N}}}\sqrt{(l^*_K)^2/18+N^{-1/2}} \sim N^{1/4}$	
Gi	$\frac{1}{16\pi^2}\frac{1}{\sqrt{N}}\left(\frac{1+N^{-1/2}}{(l^*_K)^2/18+N^{-1/2}}\right)^3 \sim N^{-1/2}$	Reference 52

IV. ILLUSTRATIVE CALCULATIONS OF THE CRITICAL AND SCATTERING PROPERTIES

As already mentioned, the free association and thermal activation models involve different numbers of free energy parameters that control the assembly process. While the simpler $\mathcal{FA}$ model is described in terms of the enthalpy Δh_p and entropy Δs_p of polymerization, the specification of the $\mathcal{A}$ model also requires including the free energy parameters (the enthalpy Δh_a and entropy Δs_a) for monomer activation. In addition to depending on these polymerization parameters, the specific thermodynamic properties depend on temperature T, the initial monomer concentration ϕ^o_1, and the van der Waals interaction ϵ_{FH}.

Calculations in the present paper are performed using the representative values $\Delta h_p = -35$ kJ/mol and $\Delta s_p = -92$ J/(mol K) which are comparable to those determined in previous experimental studies of living polymerization in poly(α-methylstyrene) solutions.[55,56] The polymerization temperature T_Φ (inflection point in Φ as a function of temperature) estimated employing these free energy parameters is typically not far above room temperature, and similar order of magnitudes for Δh_p and Δs_p have been quoted for other model fluids exhibiting equilibrium polymerization.[55–57] The lattice coordination number z is taken as $z=6$ (appropriate to a three-dimensional cubic lattice), and the effective interaction energy ϵ_{FH} is selected as $\epsilon_{\text{FH}}/k_B = 302$ K, again following the choice employed in earlier papers.[38–41] The additional free energy parameters for the activation model $\mathcal{A}$ are specified relative to those adopted for

the corresponding polymerization parameters through the reduced free energy parameters $\sigma \equiv \Delta h_a / \Delta h_p$ and $\eta \equiv \Delta s_a / \Delta s_p$. Taking $\sigma = 0$ and $\sigma = 1$ (with η restricted to unity) corresponds, respectively, to the low and high activation models discussed previously[38] in which the equilibrium constant K_a for activation, respectively, is low ($K_a = 1.67 \times 10^{-5}$) and independent of temperature for $\sigma = 0$ and is high for $\sigma \simeq 1$.

A small K_a implies low and relatively high concentrations of activated and nonactivated monomers, respectively, at the transition temperature. Within the reaction scheme defined by Eqs. (11)–(13) for the $\mathcal{A}$ model, the activated species M_1^* reacts only with unactivated monomers M_1 to form dimers, but M_1^* does not participate in the futher propagation steps. Chain growth is taken as occurring exclusively through the addition of M_1 to existing polymers M_i ($i \geqslant 2$). Thus, the resulting degree of polymerization in the fully polymerized state is relatively high for the low activation model. In contrast, the high activation model ($\sigma = 1$) is characterized by an equilibrium constant $K_a(T_p)$ at the polymerization temperature T_p that is greater than unity, which implies that almost all monomers become converted into the activated state, so that chain growth cannot proceed further due to the low concentration of the unactivated M_1 species. Consequently, the degree of polymerization is limited, and the polymerization process does not significantly affect the critical behavior of associating solutions for the high activation model.

The relative magnitude of K_a is not the only factor that governs the critical parameters in the $\mathcal{A}(\sigma, \eta)$ model, however. An interesting feature of this model for $\sigma = 1$ is that the critical composition ϕ_c becomes insensitive to the magnitude of Δh_p in the limit of large Δh_p. Specifically, ϕ_c saturates to a constant whose value generally depends only on the ratio η of the entropies of activation and polymerization. When $\eta = 1$, the critical composition ϕ_c is close to 1/2, but it decreases towards zero as η becomes larger. Consequently, the entropy ratio η in the $\mathcal{A}(\sigma = 1, \eta)$ model regulates the average chain length at low temperatures and hence plays a role similar to the initiator concentration in living polymerization systems.[39] As shown below, this strong dependence of the polymerization process on η provides a powerful means to control the polymerization index of self-assembled polymers within the $\mathcal{A}(\sigma = 1, \eta)$ model. While the calculations of critical parameters are presented for both the $\mathcal{A}_1 \equiv \mathcal{A}(\sigma = 1, \eta)$ and $\mathcal{A}_0 \equiv \mathcal{A}(\sigma = 0, \eta)$ activation models for brevity, the computational analysis for the variation of the Ginzburg number with the associating interaction Δh_p is limited to the $\mathcal{A}_0$ model since this model suffices to exemplify the more interesting general behavior that ensues when the average degree of polymerization is large near the critical point.

A. Basic critical parameters (T_c, ϕ_c, and L_c)

The critical scattering properties of equilibrium polymer solutions depend on the critical temperature T_c, critical composition ϕ_c, and other basic critical properties of these solutions (e.g., the average degree of polymerization L_c at the critical point for phase separation). Many of these basic critical properties have been examined in our recent papers[38–41] in order to uncover identifying characteristics of particular polymerization models that might be helpful in the interpretation of experimental data. This section includes a brief review of those critical properties necessary for the analysis of scattering properties and Gi and for comparisons with properties of ionic fluids. The calculations illustrate the basic nature of phase boundaries that occur in these fluids, the relation of these phase boundaries to the transition lines describing the polymerization transition, and the dependence of critical properties (T_c, ϕ_c, and L_c) on the relative strength h_ϵ of the directional association interaction and the van der Waals interaction through the dimensionless quantity $h_\epsilon \equiv (\Delta h_p / R) / \epsilon_{\mathrm{FH}}$ (where R is the gas constant).

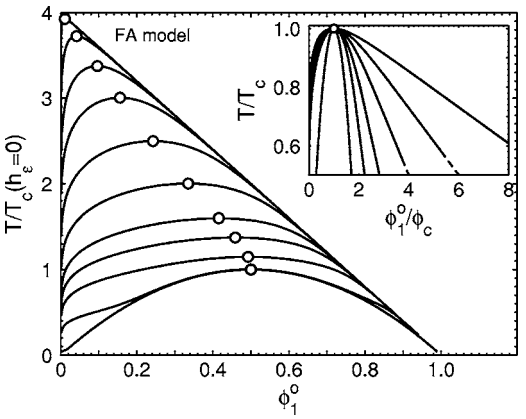

FIG. 1. Variation of the spinodal curves for freely associating polymer solutions with the dimensionless sticking energy $h_\epsilon \equiv (|\Delta h_p|/R)/(2\epsilon_{\mathrm{FH}})$. The curves from top to bottom refer to $h_\epsilon = 32$, 24, 18, 14, 10, 7.0, 5.0, 4.0, 3.0, 1.6, and 0.20 and have been computed assuming that all the polymers are completely flexible chains. The temperature scale is normalized by the critical temperature $T_c(h_\epsilon = 0)$ of the system in the absence of polymerization, and circles denote the positions of the critical points. The effective monomer-solvent interaction energy ϵ_{FH} and the entropy of polymerization Δs_p are fixed as $\epsilon_{\mathrm{FH}} = 302$ K and $\Delta s_p = -92$ J/(mol K). The inset replots the spinodal curves in terms of the reduced variables T/T_c and ϕ_1^o/ϕ_c, where T_c and ϕ_c denote the critical parameters for the system with interaction h_ϵ. The dashed curves are extrapolations to the higher composition regime where numerical instabilities make the determination of the spinodal curves difficult.

The spinodal curves are directly calculated from Eq. (10) and the critical temperatures, and critical compositions can then be determined from the extrema in the spinodals.[38,40] Since our previous studies[40] of the competition between phase separation and equilibrium polymerization emphasize *living polymerization* systems with a low concentration of initiator, we focus here instead on the critical properties of the rather different classes of associating fluids exhibiting activated polymerization or free association. Figure 1 presents examples of spinodal curves $T = T(\phi_1^o)$ calculated for a family of freely associating polymer solutions that are specified by different values of h_ϵ. As the dimensionless sticking energy h_ϵ is increased, the polymers become progressively longer at the critical point. Polymerization has little effect on the shape of the phase boundary when h_ϵ is small, but the phase boundary progressively resembles that for a high molar mass polymer solution as h_ϵ is increased. The temperature scale in Fig. 1 is normalized by the critical temperature $T_c(h_\epsilon = 0)$ of the system in the absence of polymerization in

order to visualize better the influence of h_ϵ on T_c. Association clearly makes the fluid less miscible, i.e., leads to a higher T_c. In the limit $h_\epsilon \to \infty$, the ratio of critical temperatures $T_c(h_\epsilon)/T_c(h_\epsilon=0)$ approaches 4, which equals the ratio of the theta temperature $T_\theta(h_\epsilon=0)$ (at which the monomer-solvent second virial coefficient vanishes) to the critical temperature $T_c(h_\epsilon=0)$ of the monomer-solvent mixture.[58] The constraint that the critical temperature T_c of a polymer solution must be less than the theta temperature T_θ for the monomer-solvent system ultimately limits how much $T_c(h_\epsilon)$ can be altered by particle association, and this saturation effect is apparent in Fig. 1. However, when ϵ_{FH} and Δh_p are *coupled* through a dependence on another molecular parameters, as in the Stockmayer fluid (SF), the ratio $T_c(h_\epsilon)/T_c(h_\epsilon=0)$ can exceed the limiting value shown in Fig. 1.[35]

B. Some considerations relevant to experimental observations

An interesting question at this juncture is how much the predicted phase boundaries resemble those of real associating fluids, such as the ionic and polar fluids mentioned in the Introduction. To make qualitative contact with experimental data for these systems, the spinodals in Fig. 1 are reexpressed in terms of the reduced concentration variable ϕ_1^o/ϕ_c employed in comparative studies of associating fluids ranging from simple fluids (e.g., argon) to fluorocarbon, metallic, or ionic systems where association becomes more prevelant.[9,18] The phase boundaries in the inset to Fig. 1 exhibit a remarkable resemblence to the family of phase boundaries (binodals) observed in many associating fluids (see Fig. 1 of Ref. 9). This qualitative correspondence, in conjunction with earlier experimental and simulation studies of the critical properties of ionic fluids (mentioned in the Introduction), supports the suitability of an equilibrium polymerization model to analyze the general critical behavior of associating fluids.

The sticking energy Δh_p for dipolar and charged particle fluids is proportional to the electrostatic energy for the interacting particles in their lowest energy "contact" position.[36] Since the electrostatic energy scales inversely to the static dielectric constant ϵ of the medium, Δh_p tends to be larger in the gas phase and in organic solvents where ϵ is low. High values of Δh_p can also arise for proteins and other large complex molecules that exhibit large dipole or charge induced interactions, despite the relatively high dielectric constant of water.[59] A large polarizability (as found in fullerenes and carbon nanotubes) should also lead to large values of Δh_p and thus to a propensity towards particle association.

Analyses of experimental data have often been performed under the assumption that T_p and T_Φ are the *same*,[24] but this is not generally true[60] because of the highly rounded nature of the polymerization transition in the $\mathcal{FA}$ model and in the activation models with a large K_a. The gap between T_Φ and T_p reflects the extent of transition rounding in these models. Comparison of our calculations for the $\mathcal{FA}$ model to the extensive simulation data for the SF provides an improved definition of the polymerization transition. Van Workum and Douglas[36] have found that estimates of the polymerization transition temperature, based on the temparature

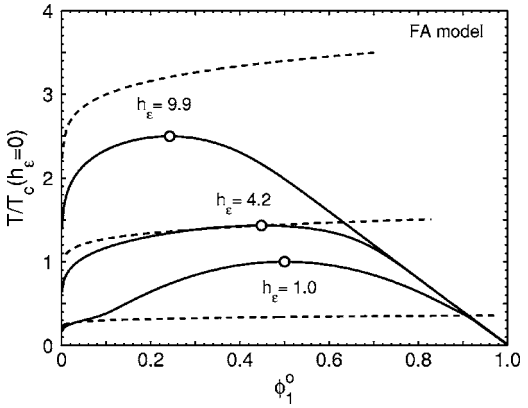

FIG. 2. Comparison of spinodal curves (solid lines) and polymerization transition lines (dashed curves) for the $\mathcal{FA}$ model. The circles mark the location of the critical points. The polymerization transition line is defined by the inflection point in the extent of polymerization $\Phi(T)$ as a function of T. Depending on the value of h_ϵ (indicated in the figure), the polymerization line may lie below or above the critical point or may coincide with the spinodal curve at the critical point. The associative interaction in the $\mathcal{FA}$ model is designated as "strong" when $h_\epsilon \gg 4$ and "weak" when $h_\epsilon \ll 4$.

T_Φ at which Φ exhibits an inflection point, yield a better description in terms of the reduced variables for the properties of the polymerizing SF (e.g., the average chain length) than those obtained by determinating the polymerization temperature as the temperature T_p at which the specific heat has a maximum. Hence, the definition in terms of T_Φ represents a better "physical" choice for ionic fluids.

C. Strong, weak, and intermediate coupling regimes of polymerization

A knowledge of the location of the polymerization transition line $T_\Phi(\phi_1^o)$ with respect to the phase boundaries governing phase separation is central to discussing the critical properties of associating fluids. When the polymerization temperature at the critical composition $T_\Phi(\phi_c)$ lies well below T_c, the critical behavior essentially reduces to that of an unassociated fluid, while when $T_\Phi(\phi_c)$ is much greater than T_c, the phase diagram should resemble that for a polymer solution. The strong coupling between polymerization and phase separation that occurs when $T_c \simeq T_\Phi(\phi_c)$ can lead to the presence of *multiple critical points* under certain circumstances and to other complex critical behavior.[38]

Figure 2 illustrates how the polymerization transition lines $T_\Phi(\phi_1^o)$ shift in relation to the phase boundaries (spinodals) as h_ϵ is varied. When h_ϵ is small (e.g., $h_\epsilon=1.0$), the polymerization line lies below the critical point, but for a large h_ϵ (e.g., $h_\epsilon=9.9$), T_Φ lies far above T_c. Thus, an intermediate h_ϵ ($h_\epsilon \simeq 4$) exists where the polymerization line intersects the spinodal curve at the critical point. We term the associative interaction "strong" when $h_\epsilon \gg 4$ and "weak" when $h_\epsilon \ll 4$. Equilibrium polymerization solutions only appear polymeric in nature when the associative interaction is relatively strong.

While the illustrative examples for the spinodals and polymerization lines in Figs. 1 and 2 refer to the $\mathcal{FA}$ model, Figs. 3–5 summarize how the pattern of critical properties becomes modified for other models of equilibrium polymer-

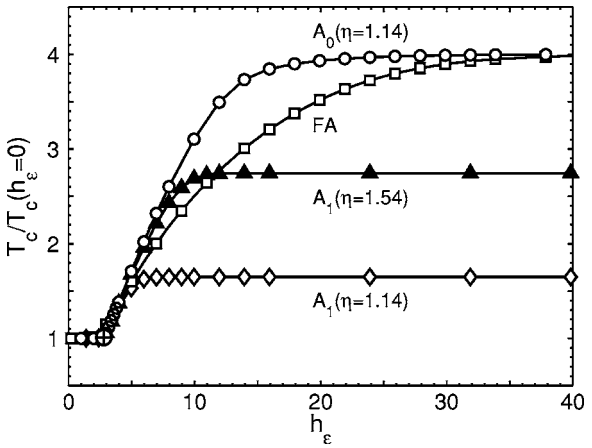

FIG. 3. The reduced critical temperature $T_c/T_c(h_\epsilon=0)$ as a function of h_ϵ for equilibrium polymerization solutions in the $\mathcal{FA}$, $\mathcal{A}_0(\eta=1.14)\equiv\mathcal{A}(\sigma=0,\eta=1.14)$, $\mathcal{A}_1(\eta=1.14)\equiv\mathcal{A}(\sigma=1,\eta=1.14)$, and $\mathcal{A}_1(\eta=1.54)\equiv A(\sigma=1,\eta=1.54)$ models defined in the text. The lines are guides to the eye. The $\mathcal{A}_0$ model exhibits two critical points for $(2.3<h_\epsilon<3.3)$ (Ref. 38).

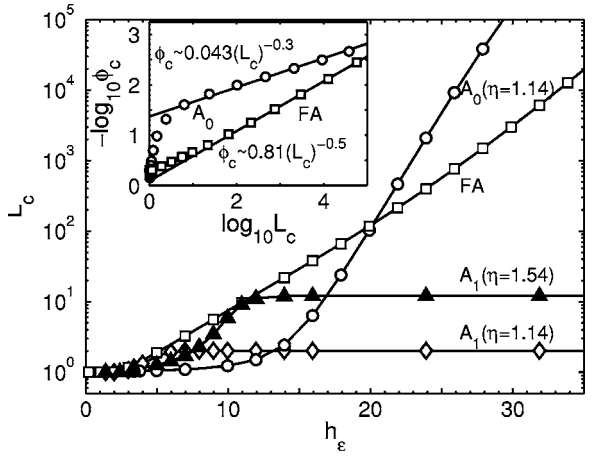

FIG. 5. Average chain length L_c at the critical point of equilibrium polymerization solutions as a function of h_ϵ for the $\mathcal{FA}$, $\mathcal{A}_0$, and $\mathcal{A}_1$ models. The lines are guides to the eye. The inset demonstrates that the critical composition ϕ_c scales as $\phi_c\sim 0.81L_c^{-0.5}$ for the $\mathcal{FA}$ model and as $\phi_c\sim 0.043L_c^{-0.3}$ for the $\mathcal{A}_0$ model.

ization. Examining the variation of critical properties (T_c and ϕ_c) with h_ϵ is helpful for understanding the physical behavior of the scattering properties described below. Figure 3 presents the relative critical temperature $T_{c,R}$ as a function of h_ϵ for the $\mathcal{FA}$, $\mathcal{A}_0$, and $\mathcal{A}_1$ models. All curves for $T_{c,R}(h_\epsilon)$ in Fig. 3 exhibit two plateau regions in which $T_{c,R}$ is insensitive to h_ϵ, but the magnitude of the second plateau in the large h_ϵ limit varies significantly between the different polymerization models. (This second plateau reflects the average degree of polymerization at the critical point as shown below). In contrast to the $\mathcal{A}_0$ and $\mathcal{FA}$ models where $T_c/T_{c,o}$ approaches 4 at high h_ϵ, the limiting ratio saturates to a lower value for the $\mathcal{A}_1$ model. The corresponding variation of the critical composition ϕ_c with h_ϵ is illustrated in Fig. 4. Apart from a regime of small h_ϵ where ϕ_c is insensitive to h_ϵ or the intermediate interaction regime where ϕ_c grows in a nonmonotonic fashion, ϕ_c decreases with h_ϵ and ultimately approaches zero ($\mathcal{FA}$ and $\mathcal{A}_0$ models) or a constant between 0 and 0.5 ($\mathcal{A}_1$ model). The tendency of the ratio $T_c/T_c(h_\epsilon=0)$ to saturate for large h_ϵ to values different than 4 and 0 is a direct consequence of the limited magnitude of L at low temperatures that emerges because of the low concentation of the nonactivated monomers that particiapte (in contrast to the activated ones) in the propagation processes.

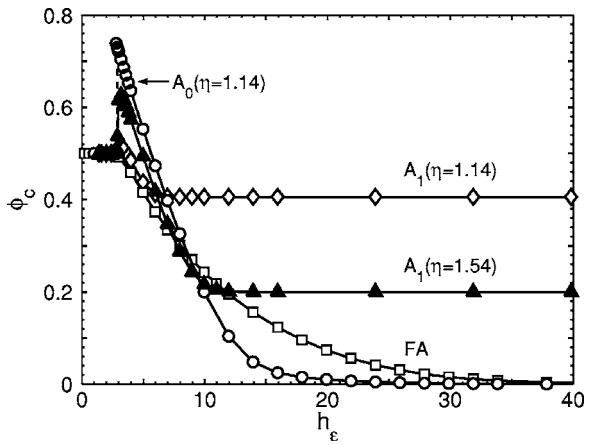

FIG. 4. The critical composition ϕ_c as a function of h_ϵ for the same models of equilibrium polymerization as described in Fig. 3. The lines are guide to the eye. Note that in the $h_\epsilon\to\infty$ limit, the critical composition ϕ_c for the $\mathcal{A}_1(\eta)$ models approaches a constant that depends on the ratio η of the entropies of activation and polymerization.

D. Average degree of polymerization L_c at the critical point

Figure 5 depicts how the average chain length L_c at the critical point changes with h_ϵ for the same polymerization models, as analyzed in Figs. 3 and 4. A large dimensionless interaction h_ϵ produces unlimited chain growth (i.e., very large L_c) for the $\mathcal{FA}$ and $\mathcal{A}_0$ models, but causes only a limited polymerization (small L_c) for the $\mathcal{A}_1$ model. In fact, the curves for $L_c(h_\epsilon)$ level off for rather low h_ϵ in the latter case, and a further increase of h_ϵ produces no change of L_c.

Knowledge of L_c also enables determining the extent to which equilibrium polymer solutions resemble ordinary polymer solutions where the polymerization is frozen in. The inset to Fig. 5 demonstrates that the critical composition ϕ_c for the $\mathcal{FA}$ model scales with L_c as $\phi_c\sim L_c^{-1/2}$, consistent with the FH theory for monodisperse polymer solutions. This agreement suggests that we can predict some quantitative aspects of the critical properties of equilibrium polymer solutions from the FH theory for monodisperse polymer solutions under certain circumstances. We further explore the limitations of this formal correspondence below.

E. Critical scattering properties and the width of the critical region

In addition to asymmetric phase boundaries and the relatively high critical temperatures that are often found for associating fluids, the scattering properties of these fluids are also quite distinct from those exhibited by simple fluids. Perhaps the most common observation is that the correlation length amplitude $\xi_{o,c}$ at the critical composition ϕ_c [see Eq. (28)] is often much larger (by an order of magnitude or more) than for simple liquids, and a similar trend is shared

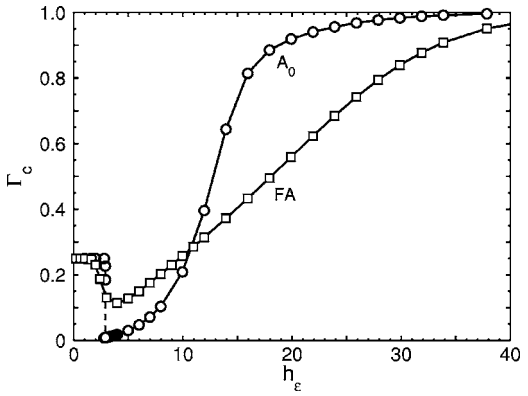

FIG. 6. Critical amplitude Γ_c of the long wave structure factor $S(0,\phi_c)$ as a function of h_ϵ for the $\mathcal{FA}$ and $\mathcal{A}_0$ equilibrium polymerization models.

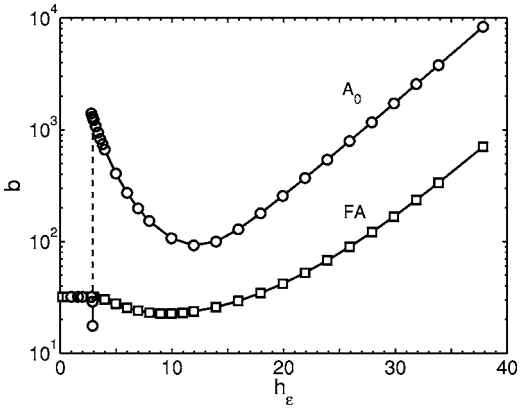

FIG. 7. Quartic coupling constant b of Eq. (23) as a function of h_ϵ for the $\mathcal{FA}$ and $\mathcal{A}_0$ equilibrium polymerization models.

by the scattering intensities. Specifically, ξ_o is typically on the order of molecular dimensions (angstrom) in simple fluids, while ξ_o of associating fluids is often reported to be on the order of nanometers and thus greatly exceeds the size of individual molecules in the fluid.[10,11,16,17,19,22] This nanoscale correlation length can naturally be understood to arise from the formation of dynamic clusters. In addition to the enhanced scattering characteristics, the larger scale of fluctuations, as set by ξ_o, leads to an increasingly broad temperature range in which mean field theory applies and to a narrower temperature range where Ising criticality is observed. (Essentially, the same phenomenon is responsible for the reduced size of the Ising critical region in binary polymer blends.[61,62]) This reduction is quantified here by calculating the Ginzburg number Gi which specifies the reduced temperature range over which mean field theory and Ising scaling should apply. The determination of Gi requires the knowledge of the critical thermodynamic properties $[T_c(h_\epsilon)$, $\phi_c(h_\epsilon)$, and $L_c(h_\epsilon)]$, as well as the critical scattering properties $[\xi_{o,c}(h_\epsilon)$, $\Gamma_c(h_\epsilon)$, and $\kappa_c(h_\epsilon)]$ that are described in the present section.

As shown in Fig. 6, the critical amplitude Γ_c for the structure factor $S(0)$ grows monotonically with h_ϵ (except for small h_ϵ where Γ_c first decreases and achieves a minimum), and Γ_c saturates to a limiting value $\Gamma_c=1$ for $h_\epsilon\to\infty$. A faster saturation of Γ_c appears for the $\mathcal{A}_0$ model which generally exhibits a greater degree of polymerization and a sharper polymerization transition than the $\mathcal{FA}$ model. The variation in these scattering properties with increasing h_ϵ is expected since an increase of h_ϵ implies an increase in the degree of polymerization at the critical point.

F. Quartic coupling constant *b* for solutions of equlibrium polymers

The quartic coupling constant b is the only parameter required for the estimation of the width of the critical regime Gi that is not directly observable experimentally. The quantity b clearly depends on molecular size asymmetry as evidenced by the strong dependence of b on the polymerization index N in Eq. (44) for ordinary polymer solutions. Since strong directional interactions naturally lead to the formation of dynamic polymeric structures, we anticipate that b should also depend strongly on the dimensionless sticking interaction h_ϵ. Figure 7 shows that b varies nonmonotonically with h_ϵ for both the $\mathcal{FA}$ and $\mathcal{A}_0$ models, and a precipitous jump and a more appreciable minimum appear for the latter case. The jump in $b(h_\epsilon)$ [and similarly a jump in $\Gamma_c(h_\epsilon)$ in Fig. 6] arises from the discountinuous variation of the critical composition ϕ_c with h_ϵ (see Fig. 4). To gain insight into the trends in Fig. 7, b is presented as a function of the average chain length L_c at the critical point and is compared to the corresponding FH estimate $b_{\mathrm{FH}}=b_{\mathrm{FH}}(L_c)$ of Eq. (44) in which the polymerization index N is replaced by L_c. Figure 8 demonstrates that $b(L_c)$ for the $\mathcal{FA}$ model agrees remarkably well with the naive FH estimate $b_{\mathrm{FH}}(N\equiv L_c)$,

$$b_{\mathrm{FH}}(L_c)=2L_c^{1/2}(1+L_c^{-1/2})^4, \tag{55}$$

over the entire range of L_c considered. This formal correspondence between permanent and dynamic polymer solutions is further supported by the scaling $\phi_c\sim L_c^{-1/2}$ (see inset to Fig. 5) noted earlier.

Unfortunately, this attractive formal correspondence fails quantitatively for the $\mathcal{A}_0$ model. First of all, ϕ_c for the $\mathcal{A}_0$

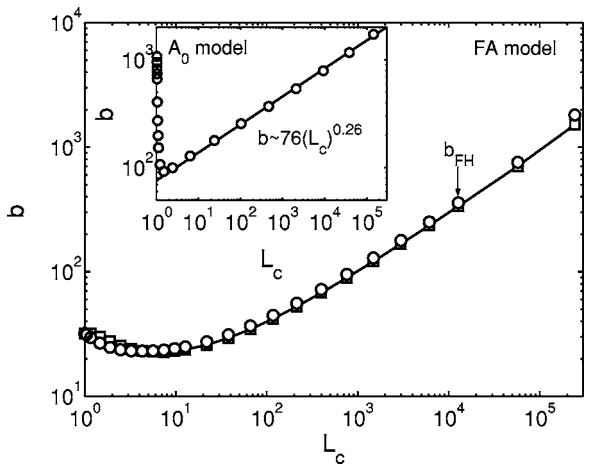

FIG. 8. Quartic coupling constant b of Eq. (23) (squares) as a function of the average degree of polymerization L_c at the critical point for the $\mathcal{FA}$ model of equilibrium polymerization. The circles denote the naive FH estimate $b_{\mathrm{FH}}(N\equiv L_c)$ from Eq. (55). The inset presents b vs L_c for the $\mathcal{A}_0$ model where Eq. (55) is no longer valid.

model scales for large L_c as $\phi_c(L_c) \simeq 0.043 L_c^{-0.30\pm0.01}$, as indicated in the inset to Fig. 5. The quartic constant b also exhibits a smaller exponent $b \simeq 76 L_c^{0.26\pm0.01}$ (see the inset to Fig. 8) than expected from the intuitive identification of equilibrium polymerization solutions with ordinary polymer solutions. Moreover, the exponents in the above power law expressions for $\phi_c(L_c)$ and $b(L_c)$ vary somewhat with the choice of free energy parameters for the $\mathcal{A}_0$ model. Despite the lack of a truly universal estimate of b based on the analogy with polymer solutions, this comparison *qualitatively explains* that the increase of b with h_ϵ in the $\mathcal{FA}$ and $\mathcal{A}_0$ models derives from the increase in $L_c(h_\epsilon)$ and suggests the existence of a scaling relation between b and L_c.

G. Square gradient coefficient κ_c, correlation length amplitude $\xi_{o,c}$, and average mean square radius of gyration $\langle R_g^2 \rangle_c$

While the critical parameters a and b are independent of the effective monomer sizes in our polymerization models, both the square gradient coefficient κ_c and the correlation length amplitude $\xi_{o,c}$ are sensitive to these size parameters through their explicit dependence of on the radii of gyration $R_{g,i}$ of the individual i-mers in the system. Consequently, calculations of κ_c and $\xi_{o,c}$ are performed for both Gaussian chains and for a family of wormlike chain models in which stiffness is tuned by choosing the fixed bond angle θ between successive bonds in the chain. Figures 9(a) and 9(b) present the square gradient coefficient κ_c [normalized by $\kappa_c(h_\epsilon=0)$ for the correponding unpolymerized system] as a function of h_ϵ for the $\mathcal{FA}$ and $\mathcal{A}_0$ models, respectively. In the former case, κ_c monotonically increases with h_ϵ, apart from the weak coupling regime where κ_c is insensitive to h_ϵ. A similar behavior has been noted before for T_c and ϕ_c and simply arises from the relatively low average degree of polymerization in this regime of low h_ϵ. However, a qualitatively different variation of κ_c with h_ϵ is found for the $\mathcal{A}_0$ model where κ_c exhibits a precipitous jump, followed by a shallow minimum, and then monotonic growth for large h_ϵ. This jump in $\kappa_c(h_\epsilon)$ appears due to the jump of the critical composition ϕ_c with h_ϵ for the $\mathcal{A}_0$ model (see Fig. 4). For both polymerization models, a larger bond angle θ in the wormlike chains leads generally to higher κ_c.

Figures 10(a) and 10(b) illustrate, respectively, the dependence of the correlation length amplitude $\xi_{o,c}$ on h_ϵ for the $\mathcal{FA}$ and $\mathcal{A}_0$ models, with $\xi_{o,c}$ in Figs. 10(a) and 10(b) normalized by its counterpart $\xi_{o,c}(h_\epsilon=0)$ for a unpolymerized monomer solvent system. The ratio $\xi_{o,c}/\xi_{o,c}(h_\epsilon=0)$ for the $\mathcal{FA}$ model exhibits a weak local minimum for small h_ϵ and then grows with h_ϵ. This minimum stems from the fact that the decrease of $\Gamma_c(h_\epsilon)$ dominates the increase of $\kappa_c(h_\epsilon)$ as a function of h_ϵ. A completely monotonic variation of $\xi_{o,c}/\xi_{o,c}(h_\epsilon=0)$ with h_ϵ is found, however, for the $\mathcal{A}_0$ model. While a typical value of $\xi_{o,c}$ for atomic and small molecule liquids is on the order[2,4] of angstroms, $\xi_{o,c}(h_\epsilon=0) \sim \mathcal{O}$ (1 Å), Figs. 10(a) and 10(b) show that this scale can be an order of magnitude larger for equilibrium polymer solutions in the strong coupling regime, $\xi_{o,c}(h_\epsilon \geqslant 10) \sim \mathcal{O}$ (1 nm). Such larger correlation length amplitudes have been observed in numerous complex fluids, often along with apparent mean field critical behavior over an appreciable temperature range.[10,11,16,17,19,22]

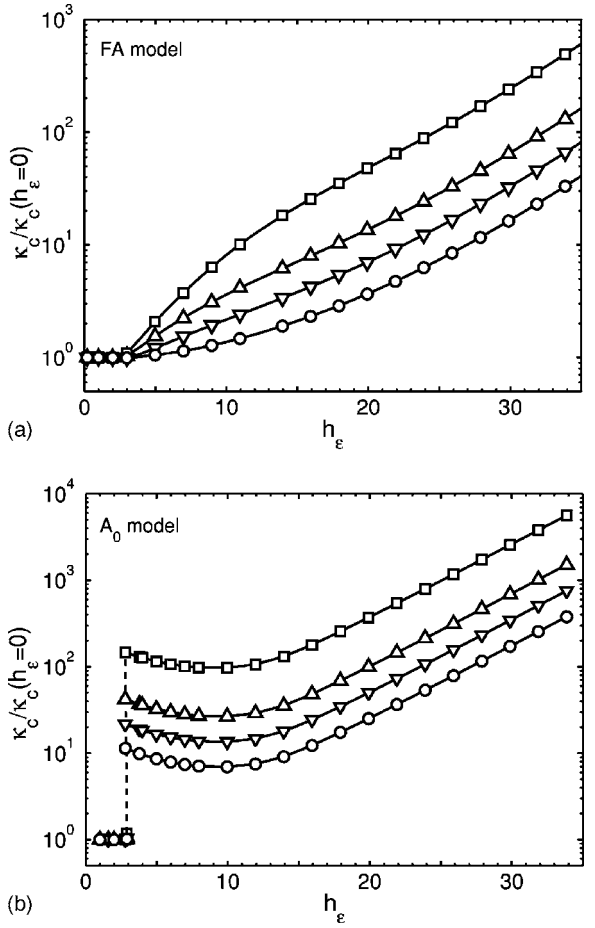

FIG. 9. (a) The reduced square gradient coefficient $\kappa_c/\kappa_c(h_\epsilon=0)$ as a function of h_ϵ for the $\mathcal{FA}$ model of equilibrium polymerization solutions. The coefficient $\kappa_c(h_\epsilon=0)$ refers to a fluid that does not exhibit polymerization. The circles correspond to Gaussian chains, while ▽, △, and □ refer to wormlike chains with the bond angles $\theta=90°$, 120°, and 150°, respectively. (b) The reduced square gradient coefficient $\kappa_c/\kappa_c(h_\epsilon=0)$ as a function of h_ϵ for the $\mathcal{A}_0$ model of equilibrium polymerization solutions. The symbols are defined as in Fig. 9(a).

The insets to Figs. 10(a) and 10(b) indicate that the average root mean square radius of gyration $\langle R_g^2 \rangle_c^{1/2}$ at the critical point increases smoothly with h_ϵ. The general trend for κ_c and $\xi_{o,c}$ to grow strongly at large h_ϵ is a direct consequence of this increase in $\langle R_g^2 \rangle_c^{1/2}$, which is parallel to the growth of L_c with h_ϵ (see Fig. 5). For comparison, the scaling relations describing κ_c, $\xi_{o,c}$, and R_g of monodisperse polymer solutions are summarized in Table I. In each case, we can predict the qualitative behavior of these properties for large h_ϵ by imposing the limit $N \to \infty$ in the corresponding expressions for critical properties of ordinary polymer solutions and by identifying N with L_c. Note that the growth of $\langle R_g^2 \rangle_c^{1/2}$ with h_ϵ is substantially more rapid that the growth of $\xi_{o,c}$. This difference can readily be concluded from the critical parameters of ordinary polymer solutions (see Table I) where $\xi_{o,c} \sim (R_g)^{1/2}$.

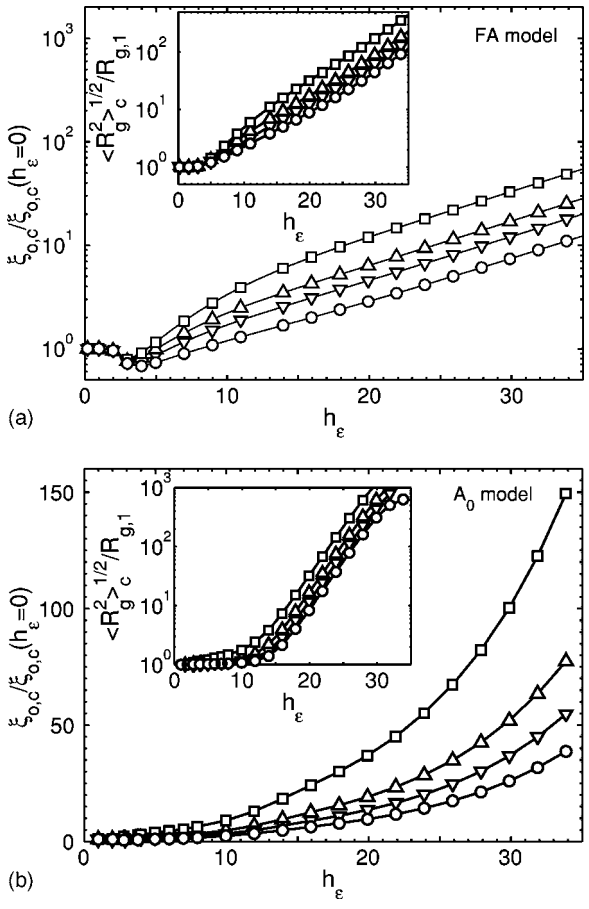

FIG. 10. (a) The reduced correlation length amplitude $\xi_{o,c}/\xi_{o,c}(h_\epsilon=0)$ as a function of the dimensionless interaction h_ϵ for the $\mathcal{FA}$ model of equilibrium polymerization solutions. The circles correspond to Gaussian chains, while ▽, △, and □, refer to wormlike chains as in Fig. 9(a). The inset presents the average root mean square radius of gyration $\langle R_g^2\rangle_c^{1/2}$ at the critical point as a function of h_ϵ for the same polymer chain models as in the main figure. $\langle R_g^2\rangle_c^{1/2}$ is normalized by the radius of gyration $R_{g,i=1}$ for a monomer. (b) The relative correlation length amplitude $\xi_{o,c}/\xi_{o,c}(h_\epsilon=0)$ as a function of h_ϵ for the $\mathcal{A}_0$ model. The symbols are defined as in Fig. 9(a), and the inset presents the average root mean square radius of gyration $\langle R_g^2\rangle_c^{1/2}$ [normalized as in Fig. 10(a)] as a function of h_ϵ.

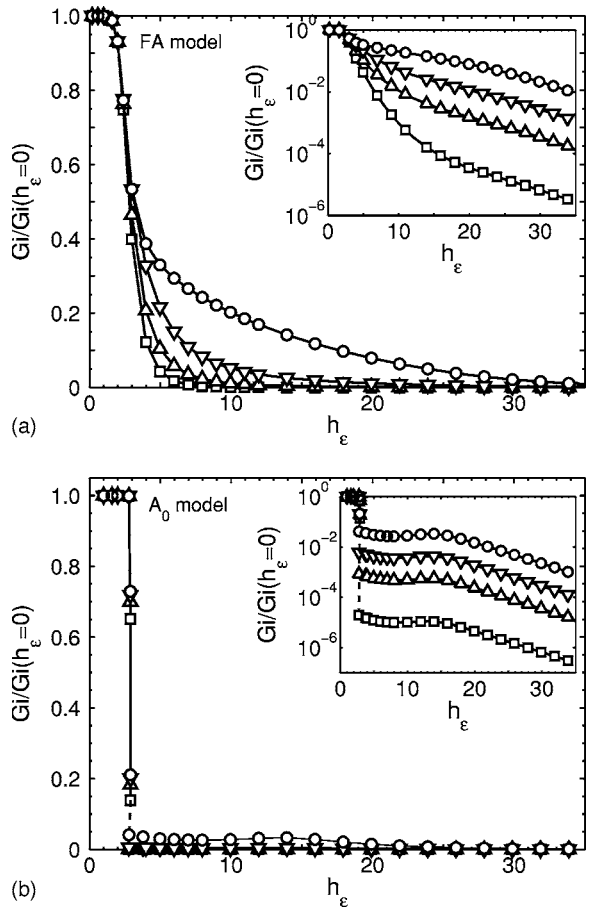

FIG. 11. (a) The Ginzburg number Gi as a function of h_ϵ for the $\mathcal{FA}$ model of equilibrium polymerization using the notation of Fig. 9(a). The Ginzburg number Gi is normalized by the value of $\mathrm{Gi}(h_\epsilon=0)$ for a monomer-solvent system [$\mathrm{Gi}(h_\epsilon=0)\simeq 0.0063$]. The inset presents data in a semilogarithmic format to accentuate the rapid decrease of $\mathrm{Gi}/\mathrm{Gi}(h_\epsilon=0)$ in the high h_ϵ limit. (b) The Ginzburg number Gi as a function of h_ϵ for the $\mathcal{A}_0$ model of equilibrium polymerization. The symbols are defined as in Fig. 9(a).

H. Width of the critical regime of equilibrium polymerization solutions

Having determined the critical equilibrium and scattering properties for our models of equilibrium polymer solutions, we now estimate how these properties affect the width of the Ising critical regime, and we check whether these calculations can explain the low experimental values of Gi $\leqslant 10^{-4}$ for nonaqueous ionic fluids.[63] A low Gi of this magnitude implies that the fluid is "effectively mean field" in character because of current limitations on the control of temperature, the influence of gravitational effects, and other complications that obviate measurements at smaller reduced temperatures τ. All previous attempts to elucidate the origin of these small Gi values in ionic fluids have been "unconvincing."[63] Since equilibrium polymerization is prevalent in ionic fluids,[31,32] these issues can be addressed from a qualitative standpoint here by using the equilibrium polymerization theory.

Figures 11(a) and 11(b) present the Ginzburg number Gi (normalized by Gi for a binary mixture of small molecules) as a function of h_ϵ. The circles refer to Gausssian chains, whereas the symbols (▽, △, and □) correspond to wormlike chains with bond angles $\theta=90°$, 120°, and 150°, respectively. The reduced Ginzburg number for freely associating polymer solutions drops from unity to small values where the rate of decline is weaker for Gaussain chains. To better appreciate the magnitude of $\mathrm{Gi}/\mathrm{Gi}(h_\epsilon=0)$, the inset presents the data in semilogarithm format. A similar behavior of Gi for solutions of semiflexible polymers emerges for the $\mathcal{A}_0$ model where $\mathrm{Gi}/\mathrm{Gi}(h_\epsilon=0)$ decreases precipitously from unity to small values [delineated in the inset to Fig. 11(b)] as h_ϵ increases. A shallow local maximum occurs in a region of intermediate h_ϵ. All polymerization models in the strong coupling regime exhibit a monotonic decrease in $\mathrm{Gi}/\mathrm{Gi}(h_\epsilon=0)$, and this ratio becomes on the order of 10^{-3}–10^{-6} (depending on the angle θ) for $h_\epsilon\simeq 35$. Thus, the formation of long chains, due to a strong associative interaction Δh_p relative to the van der Waals interaction, leads to a generic tendency for the critical regime to become small and ultimately unobservable for large h_ϵ. Variation of chain stiffness (persistence length) of the self-assembled polymers strongly affects the rate of decrease of Gi, however.

V. CONCLUSIONS

We systematically explore how polymerization affects the scattering properties of a fluid exhibiting equilibrium aggregation. Composition fluctuations associated with phase separation are superimposed on the dynamic clustering, and the coupling between polymerization and phase transition modifies the width of the critical regime, an important feature of many complex fluids (ionic fluids, microemulsions, micellular fluids, and polar liquids, and protein solutions) where particle clustering is prevalent. In particular, we calculate the scattering length and correlation length of a polymerizing liquid by using the random phase approximation. The scattering length is then employed to evaluate the Ginzburg number Gi describing how the thermodynamic and scattering properties influence the width of the Ising critical regime for phase separation. The polymerization models considered include the idealized freely associating ($\mathcal{FA}$) model in which chain segments can associate to form chains at equilibrium without constraints and an activated polymerization model $\mathcal{A}(\sigma,\eta)$ where chain polymerization is initiated by an activated process as in the polymerization of sulfur. The living polymerization system (chemically activated equilibrium polymerization) is not considered since the thermodynamic properties for this case are quite similar to those for activated polymerization where the initiator concentration plays a role analogous to the eqilibrium constant for activation in the $\mathcal{A}$ model.

Our calculations indicate that both the scale ξ and intensity $S(0)$ for compositional fluctuations become enhanced by polymerization, and the shape of the phase boundaries approaches those of increasing molecular mass polymer solutions as the association enthalpy Δh_p for polymerization increases relative to the strength ϵ_{FH} of the van der Waals interactions. This increase of the correlation amplitude ξ_o with $h_\epsilon \equiv (|\Delta h_p|/R)/(2\epsilon_{\mathrm{FH}})$ is also reflected in an increase of the average chain length and the chain radius of gyration at the critical point. These quantities are found to vary over one to two orders of magnitude, depending on the sticking interaction h_ϵ, so that the scale and intensity of composition fluctuations can be much larger in these complex fluids than in simple nonassociating fluids. Our calculations for the width of the critical regime (Gi) use this scattering information and indicate the general approach to a vanishingly small temperature range of Ising criticality for a large h_ϵ. However, the approach to this limiting behavior can be nonmonotonic and sensitive to the polymerization model.

Although the present paper does not describe the Ising critical regime where mean field theory breaks down, the properties calculated are required for a generalized crossover treatment of both the mean field and Ising critical regimes.[27–29] In particular, careful studies of the criticality of ordinary polymer solutions indicate that a sharp change in the scattering properties occurs when the correlation length ξ for the composition fluctuations becomes larger than $\langle R_g^2/3\rangle^{1/2}$, and the "mesoscopic characteristic scale" ξ_o of the theory has been clearly identified with $\langle R_g^2/3\rangle^{1/2}$. The same correspondence $\xi_o \leftrightarrow \langle R_g^2/3\rangle^{1/2}$ makes sense for associating fluids and allows us to predict critical properties over the entire accessible temperature range. While a treatment of the Ising and crossover regimes is beyond the scope of the present paper, our theory has conceptual value for understanding the emergence of these new characteristic scales that have been observed for a range of important complex fluids (nonaqueous ionic fluids,[64] metal ammonium salt mixtures,[10,11] etc.[13–15]).

Our illustrative calculations qualitatively accord with numerous observations for complex fluids for which large scale correlation length amplitudes and narrow regimes of Ising criticality have been observed. The calculations thus provide a natural framework for interpreting these observations and for determining the interaction parameters describing particle self-assembly processes that compete with phase separation.

Although substantial fragmentary data are available for the critical properties of associating fluids and although these data qualitatively accord with our model calculations, currently only limited data are suitable for quantitative comparison. Appropriate experimental systems for such a comparison must clearly conform to equilibrium polymerization systems and should simultaneously undergo phase separation in experimentally accessible temperature ranges. Systems of this kind would include living polymer systems,[65,66] such as sulfur,[67] and perhaps wormlike micelle solutions. Experimental studies of these systems are much more difficult than those of ordinary critical fluids because the polymerization transition lines must be determined relative to the phase boundaries for phase separation. Studies of even the polymerization transition lines for equilibrium polymerizing fluids are still rather limited.[55–57,65,66]

Recently, we have established that equilibrium polymerization theory provides a good description of the critical temperatures and compositions of the Stockmayer fluid model of dipolar fluids. The polymerization transition lines from computer simulations for this system conform remarkably well to those derived from the $\mathcal{FA}$ model.[36,68] In order to extend this comparison to include the scattering properties, it is necessary to generate new simulations focusing on the scattering properties of these systems and to employ improved sampling methods as used in recent estimates of the polymerization transition lines.[36] These simulations are currently in progress.[69] We also plan to extend our equilibrium polymerization model of the Stockmayer fluid to describe recent simulations for the restrictive primitive model (charged hard sphere fluids with equal numbers of positive and negative ions), generalized to include van der Waals interactions.[70] The development of a fully quantitative theory for the critical properties of associating fluids evidently requires significant further analytic, simulation, and experimental studies.

ACKNOWLEDGMENTS

This work is supported, in part, by NSF Grant No. CHE 0416017. Helpful comments by Mikhail Anisimov are acknowledged.

APPENDIX A: WORMLIKE CHAIN MODEL

The wormlike chain is defined as the limiting continuous chain generated from a discrete chain composed of n_b freely

rotating bonds of length l_b and fixed bond angle θ by imposing the limits $l_b \to 0$ and $\theta \to \pi$, while keeping both $l_b/(1+\cos\theta) \equiv (2\lambda)^{-1}$ and $n_b l_b \equiv L_w$ constant. The length $(2\lambda)^{-1}$ is termed the *persistence length*. The radius of gyration $R_{g,i=1}$ for a (structured) monomer is estimated by using simple physical arguments (see Sec. III) as

$$R^*_{g,i=1} \equiv \frac{R_{g,i=1}}{a_{\text{cell}}} = \sqrt{3}. \tag{A1}$$

In order to determine the bond length l_b in the most consistent way, we invoke the general definition of $R^2_{g,i}$,[71,72]

$$R^2_{g,i} = \frac{1}{i^2}\sum_{j}^{i}\sum_{k>j}^{i} R^2_{jk}, \tag{A2}$$

where i is the number of monomers in the chain, j and k label a pair of monomers, and R_{jk} is their separation. Using this definition to evaluate $R_{g,i=2}$ yields

$$R^2_{g,i=2} = \tfrac{1}{4} l_b^2. \tag{A3}$$

Equating the right hand sides of Eqs. (A3) and (42) for $i=2$ provides the relation between l_b and the Kuhn length l_K of the Guassian chains,

$$l_b = \frac{2}{\sqrt{3}} l_K. \tag{A4}$$

For our choice of $l_K = 2R_{g,i=1} = 2\sqrt{3}a_{\text{cell}}$, the bond length l_b of the wormlike chains equals

$$l^*_b \equiv l_b/a_{\text{cell}} = 4. \tag{A5}$$

The radii of gyration $R^*_{g,i} = R_{g,i}/a_{\text{cell}}$ of the wormlike i-mer chains ($i \geqslant 3$) can be computed by approximating the sums in Eq. (A2) by integrals. The general formula

$$(R^*_{g,i})^2 = (l^*_b)^2\left[\frac{i}{6\lambda l_b} - \frac{1}{4(\lambda l_b)^2} + \frac{1}{4(\lambda l_b)^3 i} + \frac{1}{8(\lambda l_b)^4 i^2}(e^{-2\lambda l_b i} - 1)\right] \tag{A6}$$

is cited in the literature.[72] After simple algebra, Eq. (A6) is written in a form more convenient for further analysis,

$$(R^*_{g,i})^2 = (l^*_b)^2\left[W_0 + W_1 i + W_2\frac{1}{i} - W_3\frac{1}{i^2} + W_3\frac{e^{-2\Lambda i}}{i^2}\right], \quad i \geqslant 3, \tag{A7}$$

where the coefficients $\{W_j\}$ $(j=0,1-4)$ are functions of the product $\Lambda \equiv \lambda l_b$,

$$W_0 \equiv -\frac{1}{4\Lambda^2}, \quad W_1 \equiv \frac{1}{6\Lambda}, \quad W_2 \equiv \frac{1}{4\Lambda^3}, \quad W_3 \equiv \frac{1}{8\Lambda^4}. \tag{A8}$$

Upon substituting Eqs. (A1), (A3), (A5), and (A7) into Eq. (38) and upon performing the summations over i, the dimensionless square gradient coefficient $\kappa^* = \kappa/a^2_{\text{cell}}$ emerges as

$$\kappa^* = \frac{(1/3)\Sigma_{i=1}^{\infty}[i\phi_i(R^*_{g,i})^2]}{(\Sigma_{i=1}^{\infty} i\phi_i)^2} + \frac{(1/3)(R^*_{g,s})^2}{1-\phi} = \frac{\phi_1 + \phi^*_1 + (16/3)[CA^2 + W_0 s_0 + W_1 s_1 + W_2 s_2 - W_3 s_3 + W_3 s_4]}{s^2} + \frac{1}{1-\phi}, \tag{A9}$$

where

$$s \equiv \sum_{i=1}^{\infty} i\phi_i = \phi_1 + \phi^*_1 + \sum_{i=2}^{\infty} i\phi_i = \phi_1 + \phi^*_1 + \frac{CA^2(A^2 - 3A + 4)}{(1-A)^3}, \tag{A10}$$

$$s_0 \equiv \sum_{i=3}^{\infty} i\phi_i = \frac{CA^3[4A^2 - 11A + 9]}{(1-A)^3}, \tag{A11}$$

$$s_1 \equiv \sum_{i=3}^{\infty} i^2\phi_i = \frac{CA^3(-8A^3 + 31A^2 - 44A + 27)}{(1-A)^4}, \tag{A12}$$

$$s_2 \equiv \sum_{i=3}^{\infty} \phi_i = \frac{CA^3(-2A + 3)}{(1-A)^2}, \tag{A13}$$

$$s_3 \equiv \sum_{i=3}^{\infty} \frac{\phi_i}{i} = \frac{CA^3}{1-A}, \tag{A14}$$

and

$$s_4 \equiv \sum_{i=3}^{\infty} \frac{e^{-2\Lambda}}{i}\phi_i = \frac{CY^3}{1-Y}, \tag{A15}$$

with

$$Y \equiv Ae^{-2\Lambda}, \quad \Lambda \equiv \lambda l_b.$$

Equation (A9) applies to both the $\mathcal{FA}$ and $\mathcal{A}$ models, but in the former case, the concentration ϕ^*_1 of activated monomers is set to zero in Eq. (A9). The value κ^*_c of κ^* at the critical point emerges from Eq. (A9) when the sums s_j $(j=0-4)$ are evaluated for the critical parameters $\phi_{1,c}$, $\phi^*_{1,c}$, ϕ_c, and T_c.

APPENDIX B: AVERAGE RADIUS OF GYRATION OF EQUILIBRIUM POLYMERS

The mean-square average radius of gyration $\langle R_g^2 \rangle$ of equilibrium polymers is defined as

$$\langle R_g^2 \rangle = \frac{\Sigma_{i=1}^{\infty} (R_{g,i})^2 n_i}{\Sigma_{i=1}^{\infty} n_i}, \tag{B1}$$

where $R_{g,i}$ is the radius of gyration of an i-mer (composed of i monomers) and n_i denotes the number of chains of this species, which is related to the composition ϕ_i,

$$\phi_i = i n_i / N_l. \tag{B2}$$

Since the radii of gyration $R_{g,1}$ and $R_{g,1^*}$ of monomers M_1 and M_1^*, respectively, are estimated differently from those of polymer chains (see Sec. III), the monomer contributions to $\langle R_g^2 \rangle$ are separated from the sum in Eq. (B1). This process, in conjunction with replacing the variables n_i by the corresponding composition ϕ_i (using Eq. (B2), leads to the general expression

$$\langle R_g^2 \rangle = \frac{(R_{g,1})^2 \phi_1 + (R_{g,1^*})^2 \phi_1^* + \Sigma_{i=2}^{\infty} (R_{g,i})^2 \phi_i / i}{\Sigma_{i=1}^{\infty} \phi_i / i}, \tag{B3}$$

which is valid for both Gaussain and wormlike chains. In the former case, Eq. (B3) can easily be combined with Eq. (7) defining the average chain length L and with Eq. (42) describing the radius of gyration of an individual chain in terms of its polymerization index i and the Kuhn length l_K. Thus, the average mean square radius of gyration $\langle R_g^2 \rangle$ is obtained as

$$\langle R_g^2 \rangle = \frac{1}{6} l_K^2 L + \frac{\phi_1 [(R_{g,1})^2 - l_K^2/6] + \phi_1^* [(R_{g,1^*})^2 - l_K^2/6]}{\phi_1 + \phi_1^* + CA^2/(1-A)}, \tag{B4}$$

where $A \equiv \phi_1 K_p$, C is given by Eqs. (4) and (14) for the $\mathcal{FA}$ and $\mathcal{A}$ models, respectively, $R_{g,1} = R_{g,1^*} = \sqrt{3} a_{\mathrm{cell}}$, and $l_K = 2\sqrt{3} a_{\mathrm{cell}}$.

The average mean square radius of gyration $\langle R_g^2 \rangle$ for the wormlike chains is evaluated upon substituting the corresponding expression for $R_{g,i}$ from Eqs. (A3) and (A7) into Eq. (B3). After performing the summations, the formula for $\langle R_g^2 \rangle$ emerges as a function of the persistence length parameter λ and the bond length l_b,

$$\begin{aligned} \langle R_g^2 \rangle = {} & \frac{(R_{g,1})^2 \phi_1 + (R_{g,1^*})^2 \phi_1^*}{\phi_1 + \phi_1^* + CA^2/(1-A)} + \frac{l_b^2 C}{\phi_1 + \phi_1^* + CA^2/(1-A)} \\ & \times \left[\frac{A^2}{4} + W_0 \frac{A^3}{1-A} + W_1 \frac{A^3(-2A+3)}{(1-A)^2} \right. \\ & + W_2[-\ln(1-A) - A - A^2/2] - W_3[I_A - A - A^2/4] \\ & \left. + W_4[I_Y - Y - Y^2/4] \right], \end{aligned} \tag{B5}$$

where the coefficients $W_j(\Lambda)$ are defined in Appendix A, and where

$$I_A \equiv -\int_0^A d\zeta \frac{\ln(1-\zeta)}{\zeta}, \quad 0 < \zeta < 1,$$

$$I_Y \equiv -\int_0^Y d\zeta \frac{\ln(1-\zeta)}{\zeta}, \quad 0 < \zeta < e^{-2\Lambda},$$

$Y \equiv A e^{-2\Lambda}$, $\Lambda \equiv \lambda l_b$, and $l_b = 4 a_{\mathrm{cell}}$. The integrals I_A and I_Y cannot be expressed in terms of elementary functions and must be calculated numerically. The average mean-square radius of gyration $\langle R_g^2 \rangle_c$ at the crtitical point simply follows from Eqs. (B4) and (B5) by setting $\phi_1 = \phi_{1,c}$, $\phi_1^* = \phi_{1,c}^*$, and $L = L_c$.

[1] V. L. Ginzburg, Sov. Phys. Solid State **2**, 1824 (1960).
[2] M. A. Anisimov, S. B. Kiselev, J. V. Sengers, and S. Tang, Physica A **188**, 487 (1992).
[3] A. Kostrowicka Wyczalkowska, J. V. Sengers, and M. A. Anisimov, Physica A **334**, 482 (2004).
[4] A. Kumar, H. R. Krishnamurthy, and E. S. R. Gopal, Phys. Rep. **98**, 57 (1983).
[5] M. Fisher, Rev. Mod. Phys. **46**, 597 (1974); **70**, 653 (1998).
[6] J. C. Le Guillou and J. Zinn-Justin, J. Physique **48**, 19 (1987); R. Guida and J. Zinn-Justin, J. Phys. A **31**, 8103 (1998).
[7] M. A. Anisimov, *Critical Phenomena in Liquids and Liquid Crystals* (Gordon and Breach, Philadelphia, 1991).
[8] K. S. Pitzer, Acc. Chem. Res. **23**, 333 (1990); K. S. Pitzer, J. L. Bischoff, and J. Rosenbauer, Chem. Phys. Lett. **134**, 60 (1987); K. S. Pitzer, J. Phys. Chem. **90**, 1502 (1986); R. R. Singh and K. S. Pitzer, J. Chem. Phys. **92**, 6775 (1990).
[9] K. S. Pitzer, J. Phys. Chem. **99**, 13070 (1995).
[10] P. Chieux and M. J. Sienko, J. Chem. Phys. **53**, 566 (1970).
[11] P. Chieux, P. Damay, J. Dupuy, and J. F. Jal, J. Phys. Chem. **84**, 1211 (1980).
[12] M. Buback and E. U. Franck, Ber. Bunsenges. Phys. Chem. **76**, 350 (1972).
[13] B. M. Jaffar Ali and A. Kumar, Phys. Lett. A **237**, 257 (1998); J. Jacob, A. Kumar, S. Asokan, D. Sen, R. Chitra, and S. Mazumder, Chem. Phys. Lett. **304**, 180 (1999); B. M. Jaffar Ali and A. Kumar, J. Chem. Phys. **107**, 8020 (1997).
[14] C. Ishimoto and T. Tanaka, Phys. Rev. Lett. **39**, 474 (1977).
[15] X.-H. Guo and S.-H. Chen, Phys. Rev. Lett. **64**, 1979 (1990).
[16] K. C. Zhang, M. E. Briggs, R. W. Gammon, and J. M. H. Levelt Sengers, J. Chem. Phys. **97**, 8692 (1992).
[17] K. Hamano, N. Kuwahara, T. Koyama, and S. Harada, Phys. Rev. A **32**, 3168 (1985); A. M. Bellocq, P. Honorat, and D. Roux, J. Phys. (France) **46**, 743 (1985); H. Seto, D. Schwahn, and S. Komura, J. Chem. Phys. **99**, 5512 (1993).
[18] A. D. Kirshenbaum, J. A. Cahill, P. J. Gonigal, and A. V. Grosse, J. Inorg. Nucl. Chem. **24**, 1287 (1962).
[19] M. Corti, C. Minero, and V. Degiorgio, J. Phys. Chem. **88**, 309 (1984); V. Degiorgio, R. Piazza, M. Corti, and C. Minero, J. Chem. Phys. **82**, 1025 (1985).
[20] D. Blankschtein, G. M. Thurston, and G. B. Benedek, Phys. Rev. Lett. **54**, 955 (1985).
[21] M. E. Fisher, J. Stat. Phys. **75**, 1 (1994).
[22] H. Weingärtner and W. Schröder, Adv. Chem. Phys. **116**, 1 (2001).
[23] T. Narayanan and K. S. Pitzer, Phys. Rev. Lett. **73**, 3002 (1994); T. Narayanan and K. S. Pitzer, J. Phys. Chem. **98**, 9170 (1994); **102**, 8118 (1995).
[24] D. Seto, D. Schwahn, M. Nagao, E. Yoko, S. Komura, M. Imai, and K. Mortensen, Phys. Rev. E **54**, 629 (1996).
[25] J. Jacob, A. Kumar, M. A. Anisimov, A. A. Povodryev, and J. V. Sengers, Phys. Rev. E **58**, 2188 (1988); K. Gutkowski, M. A. Anisimov, and J. V. Sengers, J. Chem. Phys. **114**, 3133 (2001).
[26] J. Jacob, M. A. Anisimov, A. Kumar, V. A. Agayan, and J. V. Sengers, Int. J. Thermophys. **21**, 1321 (2000).
[27] M. A. Anisimov, A. A. Povodyrev, and J. V. Sengers, Fluid Phase Equilib. **158–160**, 537 (1999); M. A. Anisimov, A. A. Povodyrev, V. D. Kulikov, and J. V. Sengers, Phys. Rev. Lett. **75**, 3146 (1995); M. A. Anisimov, J. Phys. C **12**, A451 (2000).
[28] Y. B. Melnichenko, M. A. Anisimov, A. A. Povodrev, G. D. Wignall, J. V. Sengers, and W. A. Hook, Phys. Rev. Lett. **79**, 5266 (1997); M. A. Anisimov, V. A. Agayan, and E. E. Gorodetskii, JETP Lett. **72**, 578 (2000); M. A. Anisimov, A. F. Kostko, and J. V. Sengers, Phys. Rev. E **65**, 051805 (2002).

[29] M. A. Anisimov, A. F. Kostko, J. V. Sengers, and I. K. Yudin, J. Chem. Phys. **123**, 164901 (2005).
[30] N. Bjerrum, K. Dan. Vidensk. Selsk. Mat. Fys. Medd. **7**, 1 (1926); H. Friedman, J. Phys. Chem. **66**, 1595 (1962); K. S. Pitzer and D. R. Schreiber, Mol. Phys. **60**, 1067 (1987); J. M. H. Levelt Sengers and J. A. Given, *ibid.* **80**, 899 (1993); Y. Levin and M. E. Fisher, Physica A **225**, 164 (1996); K. S. Pitzer, J. Chem. Phys. **104**, 6724 (1996).
[31] A. Z. Panagiotopoulos and M. E. Fisher, Phys. Rev. Lett. **88**, 045701 (2002); Q. L. Yan and J. J. de Pablo, *ibid.* **88**, 095504 (2002).
[32] S. Bastea, Phys. Rev. E **66**, 020801 (2002); M. Gillian, B. Larsen, M. P. Tosi, and N. H. March, J. Phys. C **9**, 889 (2002).
[33] P. G. de Gennes and P. A. Pincus, Phys. Kondens. Mater. **11**, 189 (1970); P. C. Jordan, Mol. Phys. **25**, 961 (1973); M. A. Osipov, P. I. Teixeira, and M. M. T. da Gama, Phys. Rev. E **54**, 2597 (1996); P. I. Teixeira, J. M. Tavares, and M. M. T. da Gama, J. Phys. C **12**, R411 (2000); J. M. Tavares, M. M. T. da Gama, and M. A. Osipov, Phys. Rev. E **56**, R411 (2000); J. M. Tavares, J. J. Weis, and M. M. T. da Gama, *ibid.* **65**, 061201 (2002).
[34] W. H. Stockmayer, J. Phys. Chem. **96**, 4084 (1992).
[35] J. Dudowicz, K. F. Freed, and J. F. Douglas, Phys. Rev. Lett. **92**, 045502 (2004).
[36] K. van Workum and J. F. Douglas, Phys. Rev. E **71**, 031502 (2005); **73**, 031502 (2005); Macromol. Symp. **227**, 1 (2005); Mater. Res. Soc. Symp. Proc. (in press).
[37] These calculations minimize errors in nonuniversal properties, such as the critical temperature and composition, by considering the ratios of these quantities and those pertaining to a nonassociating reference fluid.
[38] J. Dudowicz, K. F. Freed, and J. F. Douglas, J. Chem. Phys. **119**, 12645 (2003).
[39] J. Dudowicz, K. F. Freed, and J. F. Douglas, J. Chem. Phys. **111**, 7116 (1999).
[40] J. Dudowicz, K. F. Freed, and J. F. Douglas, J. Chem. Phys. **112**, 1002 (2000).
[41] J. Dudowicz, K. F. Freed, and J. F. Douglas, J. Chem. Phys. **113**, 434 (2000).
[42] A. V. Tobolsky and A. Eisenburg, J. Am. Chem. Soc. **81**, 780 (1950); *ibid.* **81**, 2302 (1950); *ibid.* **82**, 289 (1960); J. Colloid Sci. **17**, 49 (1962).
[43] M. N. Artyomov and K. F. Freed, J. Chem. Phys. **123**, 194906 (2005).
[44] The theory is readily extended to cases of unequal volumes, as described in Ref. 38.
[45] Equation (4) departs from expressions given in Ref. 38 since the factor $(z-1)$ is now absorbed in Δs_p and, thus, is included in the defintion of K_p.
[46] Experiments indicate, however, that χ often contains a temperature independent portion that may significantly affect the phase behavior. This entropic portion of χ parameters arises naturally within the lattice cluster theory as a quantity directly related to the monomer structures of the components of the system (Ref. 73).
[47] A. V. Tobolsky and A. Eisenberg, J. Am. Chem. Soc. **81**, 780 (1959).
[48] J. Dudowicz, M. Lifschitz, K. F. Freed, and J. F. Douglas, J. Chem. Phys. **99**, 4804 (1993).
[49] J. Higgins and H. Benoit, *Polymers and Neutron Scattering* (Oxford University Press, New York, 1994).
[50] K. S. Schweizer and J. G. Curro, J. Chem. Phys. **91**, 5059 (1989).
[51] A. P. Andrews, K. P. Andrews, S. C. Greer, F. Boue, and P. Pfeuty, Macromolecules **27**, 3902 (1994).
[52] A. D. Mackie, A. Z. Panagiotopoulos, and S. B. Kumar, J. Chem. Phys. **102**, 1014 (1995).
[53] J. M. H. Levelt Sengers and J. V. Sengers, in *Perspectives in Statistical Physics*, edited by H. J. Raveche (North-Holland, Amsterdam, 1981), Chap. 14.
[54] A. A. Povodyrev, M. A. Anisimov, J. V. Sengers, Physica A **264**, 345 (1999).
[55] S. C. Greer, J. Phys. Chem. B **102**, 5413 (1998).
[56] S. C. Greer, Adv. Chem. Phys. **94**, 261 (1996).
[57] S. C. Greer, Annu. Rev. Phys. Chem. **53**, 173 (2002).
[58] P. J. Flory, *Principles of Polymer Chemistry* (Cornell University Press, Ithaca, 1953).
[59] W. D. B. Jenkins and Y. Marcus, Chem. Rev. (Washington, D.C.) **95**, 2695 (1995).
[60] These temperatures become equal for living polymerization systems, leading to this misinterpretation.
[61] P. G. De Gennes, J. Phys. (Paris), Lett. **38**, L441 (1977).
[62] K. Binder, J. Chem. Phys. **79**, 6387 (1983); Phys. Rev. A **29**, 341 (1984).
[63] M. E. Fisher and B. P. Lee, Phys. Rev. Lett. **77**, 3561 (1996); M. E. Fisher, J. Phys. C **8**, 9103 (1996).
[64] M. A. Anisimov, J. Jacob, A. Kumar, V. A. Agayan, and J. V. Sengers, Phys. Rev. Lett. **85**, 2336 (2000).
[65] S. C. Greer, Phys. Rev. Lett. **64**, 1983 (1990); K. M. Zheng, S. C. Greer, L. Rene Corrales, and J. Ruiz-Garcia, J. Chem. Phys. **98**, 9873 (1993).
[66] S. C. Greer, Phys. Rev. Lett. **64**, 3204 (1990).
[67] R. L. Scott, J. Phys. Chem. **69**, 261 (1965); J. A. Larkin, J. Katz, and R. L. Scott, J. Chem. Phys. **71**, 352 (1967).
[68] J. Stammbaugh, K. van Workum, J. F. Douglas, and W. Losert, Phys. Rev. E **72**, 031301 (2005).
[69] C. Miller, J. J. de Pablo, and J. F. Douglas (unpublished).
[70] A. Diehl and A. Z. Panagiotopoulos, J. Chem. Phys. **118**, 4993 (2003); J. C. Shelly and G. N. Patey, *ibid.* **103**, 8299 (1995); J. M. Romero-Enrique, L. F. Rull, and A. Z. Panagiotopoulos, Phys. Rev. E **66**, 041204 (2002).
[71] K. F. Freed, *Renormalization Group Theory of Macromolecules* (Wiley, New York, 1987).
[72] H. Yamakawa, Modern Theory of Polymer Solutions (Harper & Row, New York, 1971).
[73] K. F. Freed and J. Dudowicz, Macromolecules **31**, 6681 (1998).